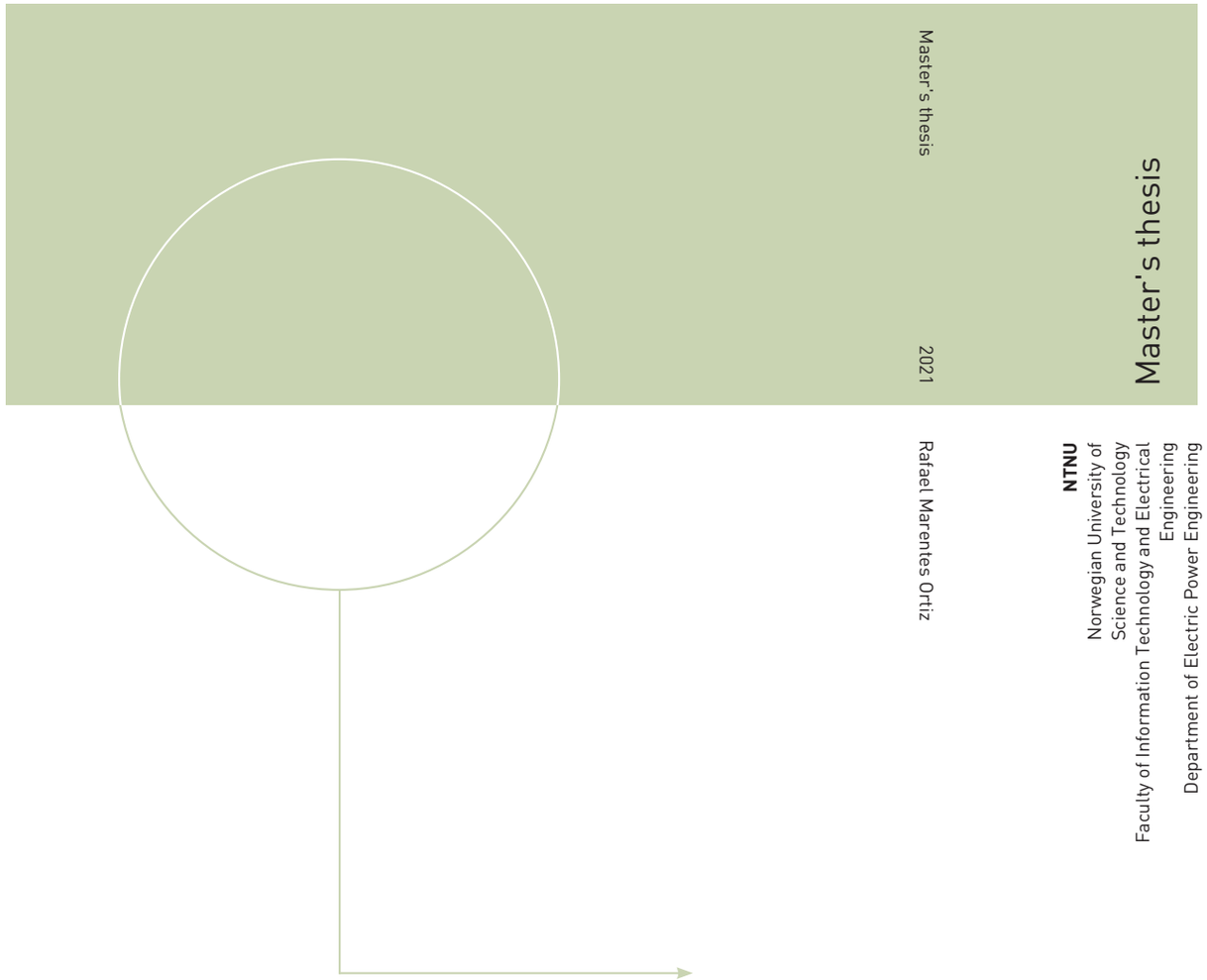

Master's thesis

2021

Rafael Marentes Ortiz

NTNU
Norwegian University of
Science and Technology
Faculty of Information Technology and Electrical
Engineering
Department of Electric Power Engineering

Rafael Marentes Ortiz

Seamless Operation Mode Change of the Inverter-based Microgrid with Robust Synchronization Loop

June 2021

NTNU
Norwegian University of
Science and Technology

NTNU
Norwegian University of
Science and Technology

NTNU
Norwegian University of
Science and Technology

Seamless Operation Mode Change of the Inverter-based Microgrid with Robust Synchronization Loop

Rafael Marentes Ortiz

Renewable Energy in the Marine Environment
Submission date: June 2021
Supervisor: Mohammad Amin

Norwegian University of Science and Technology
Department of Electric Power Engineering

Seamless Operation Mode Change of the Inverter-based Microgrid with Robust Synchronization Loop

Rafael Marentes-Ortiz

Master's thesis in Renewable Energy in the Marine Environment
Supervisor: Mohammad Amin
June 2021

Abstract

In this document a method to seamlessly change the mode of operation of microgrids connected to the grid is presented. Microgrids can work connected to the grid (grid-connected mode) or stand-alone (islanded mode), so the topic covered here is the soft transition between these modes, from grid-connected to islanded and from islanded to grid-connected. In this thesis an overview of the current situation of the integration of renewables to the grid is given and it is explained why there is a need for smooth reconnection procedures in the control of microgrids. A brief review is given on the elements of a microgrid and the design procedures for commonly used converters and their control methods. These includes boost and buck-boost converters, MPPT algorithm for PV power extraction optimization, and LCL filter design.

Some of the approaches that have been proposed in the literature are introduced and reviewed to understand the alternatives there are for reconnection methods, and to serve as a baseline to compare with the method presented here. A detailed analysis of a control block known as Robust Synchronization Loop (RSL) will be presented as an alternative to traditional Phased-Locked Loop (PLL) devices, and as the key enabler of the reconnection procedure proposed in this thesis. The RSL can (i) accurately track the grid frequency and angle, (ii) remain stable during its operation, and (iii) help in the process of synchronization.

It is shown that the reconnection capabilities of this method are comparable to the ones exhibited by the Universal Droop Control with the added resynchronization block, making it a vector control equivalent alternative. The tested microgrid model presents a stable behaviour while working in all operation modes and during the transitions between them, it also displays fast response times during errors and the ability to operate safely while unintentionally islanded. In the end it was possible to avoid any transient overcurrents as the microgrid synchronizes the voltage with the grid before either connection or reconnection.

Matlab/Simulink simulations are used to prove the mentioned capabilities; the method presented is (i) easy to configure and tune, (ii) modular, (iii) reliable and stable, and (iv) computationally light-weight.

Sammendrag

I dette dokumentet presenteres en metode for sømløs endring av driftsmåten til mikronett koblet til nettet. Mikronett kan fungere koblet til rutenettet (rutenett-tilkoblet modus) eller frittstående (øy-modus), så temaet som dekkes her er den myke overgangen mellom disse modusene, fra rutenett-tilkoblet til øy-og fra øy-til rutenett-tilkoblet. I denne oppgaven blir det gitt en oversikt over den nåværende situasjonen for integrering av fornybar energi til nettet, og det er forklart hvorfor det er behov for jevnlige tilkoblingsprosedyrer i kontrollen av mikronett. En kort gjennomgang blir gitt om elementene i et mikronett og designprosedyrene for vanlige omformere og deres kontrollmetoder. Disse inkluderer boost- og buck-boost-omformere, MPPT-algoritme for optimalisering av PV-kraftuttak og LCL-filterdesign.

Noen av tilnærmingene som er foreslått i litteraturen blir introdusert og gjennomgått for å forstå alternativene som finnes for gjenkoblingsmetoder, og for å tjene som en grunnlinje for å sammenligne med metoden presentert her. En detaljert analyse av en kontrollblokk kjent som Robust Synchronization Loop (RSL) vil bli presentert som et alternativ til tradisjonelle Phased-Locked Loop (PLL) enheter, og som nøkkelen til å gjenopprette prosedyren som er foreslått i denne oppgaven. RSL kan (i) nøyaktig spore nettfrekvensen og vinkelen, (ii) forbli stabil under drift, og (iii) hjelpe i synkroniseringsprosessen.

Det er vist at resonneksjonsfunksjonene til denne metoden er sammenlignbare med de som vises av Universal Droop Control med den ekstra resynkroniseringsblokken, noe som gjør den til et alternativ for vektorkontroll. Den testede mikronettmodellen presenterer en stabil oppførsel mens du arbeider i alle driftsmodi og under overgangene mellom dem, den viser også raske responstider under feil og evnen til å operere trygt mens du utilsiktet er øya. Til slutt var det mulig å unngå forbigående overstrøm, da mikronettet synkroniserer spenningen med nettet før tilkobling eller tilkobling igjen.

Matlab / Simulink simuleringer brukes til å bevise de nevnte evnene; metoden som presenteres er (i) enkel å konfigurere og stille inn, (ii) modulær, (iii) pålitelig og stabil, og (iv) beregningsmessig lett.

Preface

This is the final report presented during my studies in the Erasmus Mundus Renewable Energy in the Marine Environment (REM) Master in Science programme, which took place at the University of Strathclyde (semester 1), the University of the Basque Country (semester 2), and the Norwegian University of Science and Technology(semesters 3 and 4). This document was written during the last semester under the supervision of Associate Professor Mohammad Amin at NTNU in Trondheim.

I hope this report helps the reader understand the concept of microgrids, its elements, its design, and its control. The process of writing this thesis has been enriching, helping me acquire a better understanding of topics like the vector control of inverters, tuning of PI and droop controllers, and stability analysis. I hope that the information gathered here serves as my initial contribution in making it easier to integrate more renewable energy into the grid by increasing the number of alternatives available. I think that the microgrid is an important step towards the inclusion of small renewable projects, which I hope will encourage the development of tidal and wave-energy-converter systems, which have been lagging behind, but that hold great potential.

I want to thank professor Mohammad Amin for mentoring me in the field of microgrids, guiding my work during this semester, and providing me with the background and consultation material that made this work possible. Despite the uncertainties and limitations the current Covid-19 health crisis imposed, I always had the necessary means to concentrate on my task; his constant assistance and supervision were invaluable, and for this I am very thankful.

I also want to take the opportunity to thank all the people that have been with me and supported me all along: My siblings: Monica, Sofia and Alfredo; my mother, with her example of excellence, her loving presence and her frequent calls that kept me in touch; my grandparents; my godparents Danold and Monica, for their love and never-ending support; my aunt and uncle, Vicky and Angel, always motivating me in my academic pursuits; my friends, the old ones in Mexico and the new ones from all over the world, making my studies a very enjoyable period. Finally I want to thank Lissie, without whom this thesis would not have been

possible; living away from home and on your own is not easy and I owe it to her for making the good times blissful and the hard times bearable.

Contents

Figures

Tables

Code Listings

Acronyms

AC Alternating Current. iii

BES Battery Energy Storage. iii

BESS Battery Energy Storage System. iii

CCM Continuous Current Mode. iii

DC Direct Current. iii

DG Distributed Generation. iii

DU Dispatch Unit. iii

ESS Energy Storage System. iii

FACTS Flexible AC Transmission System. iii

HV High Voltage. iii

LV Low Voltage. iii

LVRT Low Voltage Ride Through. iii

MPP Maximum Power-Point. iii

MPPT Maximum Power-Point Tracking. iii

PCC Point of Common Coupling. iii

PI Proportional-Integral. iii

PLL Phase-Locked Loop. iii

PV Photovoltaic. iii

PWM Pulse Width Modulation. iii

RSL Robust Synchronization Loop. iii

SPWM Sinusoidal Pulse Width Modulation. iii

Chapter 1

Introduction

This introductory chapter is intended to help the reader understand the context and objectives of this report. It offers an overview of the concept of a microgrid in the context of renewable energy penetration and its challenges. Finally, it specifies the scope and delimitations of the work and outlines the structure and content of the thesis.

1.1 Background and Motivation

Energy demands keep increasing around the world, meanwhile climate change remains the biggest concern of our era. From 2010 to 2018 photovoltaic energy has increased almost twenty-fold from 30 TWh to around 600 TWh, while wind has increased from 350 TWh to nearly 1,400 TWh. And even though the interest for renewable sources is a clear trend, the share of renewables in this same period has not changed much, with a participation of about 17% [1].

The energy transition is not moving at the same pace everywhere, in Europe the participation of renewable generation is much more pronounced, with wind energy surpassing hydro generation and placing itself just below coal since 2018 [1], thanks to the development of offshore wind parks.

This sudden increase of renewable energy concentrated in specific regions, like Europe, brings some challenges to the way the electric grid is managed. The old paradigm of grid control is through the frequency regulation to sort the supply-demand balance. This method works by observing the behaviour of the frequency to understand the current state of the energy demand, as the demand increases the frequency drops due to large rotating generators having to provide part of their kinetic energy. The frequency drop is gradual due to the inertia of these large machines and is a great indicator of the state of the grid. Under this paradigm, frequency variations are not only expected, but desirable since they would warn the administrators and allow them to decide on how to respond.

In the future electric grid such paradigm would be obsolete since it is expected that the grid will be based on grid-forming inverters which lack large rotating masses that are the key element under the inertial-frequency regulation method. It is usual to find information about the low inertia of the system caused by renewable sources that get branded as incapable of frequency control, but this is far from true. Inverters are faster than the current frequency response, so fast that the imbalance which triggered the frequency variation could go undetected. It is not that inverters cannot work with the grid, it is simply that they are not being controlled in a way that is compatible with the current paradigm.

Some concepts like that of Virtual Inertia have been brought up to integrate renewable sources with the old scheme, but virtual inertia devices do not really provide the system with inertia, it simply boosts power injection to alleviate the supply-demand imbalance rather than regulate the frequency. As the penetration of renewable energy increases frequency swings will continue increasing until a transition to a different frequency control method is done. In the meantime, they will have to operate simultaneously with synchronous generators.

To work correctly with the grid, inverters have two main actions: grid-following and grid-forming. The former control the active and reactive power injected into the grid, while the latter set their own voltage and frequency. Grid-forming inverters operate in microgrids that can work by themselves in stand-alone mode, but they can also work in grid-connected mode.

1.1.1 Microgrids

A microgrid is an energy system made up of distributed generation, storage systems, and local loads in a specific location. Microgrids are self-sufficient systems, capable of providing for their own energy needs; nonetheless, they are usually connected to the main grid. There are three main characteristics of a microgrid:

- Local: energy sources and consumers are close to each other, dispensing from large transmission systems and the losses associated with transmission and distribution.
- Independent: it can run independently from the main grid and maintain its operation in case the grid is absent.
- Intelligent: it controls the overall behaviour of its components and optimizes price, reliability, pollution, etc.

The ability of the microgrid to work independently represents a huge advantage, but also a challenge. When the microgrid operates islanded, despite its voltage and frequency controls, the electric parameters drift away from the main grid ones, resulting in unwanted transitory currents that destabilize the system if

Table 1.1: IEEE 1547 standard for grid reconnections

Average Power $[MW]$	Frequency difference [Hz]	Voltage difference [pu]	Phase difference [°]
0 – 500	0.3	0.1	20
501 – 1500	0.2	0.05	15
1501 – 10000	0.1	0.03	10

reconnected. Therefore, a process must be carried out to effectively achieve the reconnection to the grid.

1.1.2 Microgrid mode transition

There have been several proposals to address the obstacles encountered when microgrids change operation modes. They vary widely from attenuation methods that reduce overcurrents and oscillations, to resynchronization techniques that ensure a match of the electric parameters at the point of common coupling (PCC), these parameters are frequency, phase, and voltage magnitude. The process by which this is achieved is known as synchronization. To supply the electric demand without interruptions, it is of the utmost importance for the microgrid to be able to operate in both modes, grid-connected and islanded, with smooth transitions between them[2, 3]. In chapter 3 some of these proposals are analysed and discussed, and some new ideas are developed and compared to the existing solutions to study their feasibility and advantages.

Even with the best controls the electric conditions will never be exactly the same for both grids, so tolerances are considered and specified in the IEEE 1547 standard summarized in table 1.1

1.1.3 Motivation

Microgrids are considered facilitators of the integration of renewable energy such as solar and wind power into the electric system, as they allow for smaller distributed generation systems to participate by bundling together, easing its management and control. By simplifying the connection of microgrids into the electric system an increase of the penetration of renewable sources is also promoted. The work presented in this document provides control tools that will help inverter based microgrids to easily integrate with today's grid. It also helps address the negative impact mode transitions have on the grid by achieving a seamless operation.

1.2 Objectives

The purpose of this thesis is to present a control strategy based on the vector control method of three-phase inverters to manage a microgrid in any operation mode. This document shows a proposal to connect a microgrid to the grid without overcurrents or power oscillations. It also illustrates how the inconveniences of traditional phase-locked loop (PLL) blocks have can be avoided by using a robust synchronization loop (RSL), whose operation is stable and the tuning straightforward. Finally, it shows its performance during simulations to prove that the desired behaviour is obtained. It is demonstrated that a microgrid behaves the way it does with a similar technique implemented on droop controllers without the disadvantage of working at off-nominal values.

The research objectives are the following:

- Propose a modified RSL block that works as a frequency reference and as a synchronizer.
- Present a new reconnection method that works with the already existent vector modulation.
- Prove the stability of the system for all operation modes.
- Understand the advantages, disadvantages and limitations of this reconnection method.

1.3 Contribution

This thesis provides new tools for the effective control of grid-connected microgrids, increasing the range of available options that address seamless reconnections. It provides a method that does not require extra equipment to be implemented as it does not need a communication network nor additional frequency measurements other than the one already used for the vector modulation technique.

In addition to this, a modified RSL block is presented, which requires a minimal setup and is easily implemented without much computational demand.

The proposed method is not only built on well understood control schemes, but is able to achieve the stability of operation observed in droop control inverters which do not rely on PLL blocks while following flawlessly the provided set-points.

Finally, the design, simulations and results were all compiled in the format of a scientific paper of which a draft is included at the end of this thesis.

1.4 Scope and Limitations

This document is focused on inverter-based microgrid seamless transition between operation modes. This study covers the behaviour of the current, voltage and power during the reconnection of the system and during absences of the grid. It is done with a simulated microgrid designed for this specific purpose during the last semester of the master. The microgrid is designed element by element and implemented on Simulink, control systems are proposed to control the different components of the microgrid, and simulations are run to study its behaviour. This document aims to improve the understanding of the control challenges of grid-tied inverters, what the current reconnection methods are, and their requirements.

This study is limited to microgrids that are interfaced by an inverter to the grid. The Distributed Generation is assumed to come from renewable sources, and connected through a DC bus, a battery energy storage system (BESS) is considered to be connected at the DC bus as well. No engines or other such machines are considered as part of the microgrid as the objective of popularizing the existence of microgrids is to promote the penetration of renewable sources. The simulations will only be numerical through Matlab/Simulink, with no real models used to test the proposed implementation. Finally, unless otherwise noted, the grid is operated at 50 Hz with no variations.

The following has been excluded from this study, as they were not the main concern of the study.

- Battery dynamics and state of charge effects in the potential of the battery.
- PV system events, e.g. faults or partial shading.

1.5 Thesis Structure

This document is organized in three levels, starting with numbered chapters which are structured in sections and subsections with the form X.Y.Z, where X is the number of the chapter, Y the number of the section and Z, the subsection. This number is followed by the name like “Thesis Structure” which is section 5 of chapter 1. Codes, tables, and figures are numbered with the form X.A, where X is again the chapter and A increases with each instance of the object, they are not affected by sections or subsections.

The bibliography format is the one defined in NTNU’s thesis template which is the style defined by the IEEE. References to elements of the bibliography are identified by numbers in square brackets, while references to elements of the report are identified by numbers in parenthesis.

This thesis consists of 7 chapters that range from the introduction to the conclusions and includes appendices with relevant information, figures or documents. Each chapter begins with a brief description of its content, these have been copied here to provide an outline of the structure of the report.

Chapter 2 presents the theoretical background of each of the components considered for the simulation of the microgrid and its control. For the electronic implementation of converters and filters the design equations are presented and the control methods discussed.

Chapter 3 serves as a literature review on reconnection methods for microgrids. It aims to familiarize the reader with the current approaches, their achievements, advantages, and drawbacks. It is also intended to serve as a point of comparison when measuring the performance of the method presented in this report.

Chapter 4 introduces the microgrid model used to test the proposed implementation. The system parameters are defined, and the design of each element is shown and justified.

Chapter 5 presents the tuning and control of the inverter. The control blocks are explained in detailed along with the tuning procedure and defined parameters. The structure of each control loop is studied and an overview of the operation modes of the microgrid is presented. In this chapter the necessary modifications needed to use the RSL as a synchronization block are presented.

Chapter 6 analyses the results from the simulation of the microgrid with the structure and control described in the previous chapters. The behaviour of the current is discussed, and the stability of the system is studied.

Chapter 7 contains the conclusions drawn from the observed performance and the analysis of the results. It presents how the objectives of this work are achieved and presents some final remarks regarding the possible applications and limitations of the proposed scheme. It concludes with possible topics for further research based on the delimitations of this study.

Appendix A has the parameters of the microgrid presented in tables for the main components.

Appendix B displays the Simulink models of each of the components and their respective controls.

Appendix C includes the article generated from the work of this thesis.

Chapter 2

Background Theory

This chapter presents the theoretical background of each of the components considered for the simulation of the microgrid and its control. For the electronic implementation of converters and filters the design equations are presented and the control methods discussed.

2.1 Photovoltaic System

Considering that global energy demands have increased continuously over the last decades, and the environmental concerns that arise from it, new alternative energy sources have become more popular. Solar Photovoltaic generation is one of the renewable sources that are used for global warming mitigation by avoiding the emission of greenhouse gases. The size of PV installations range from individual panels and systems integrated within buildings to large scale stations of hundreds of kilowatts or even megawatts. Most of the Photovoltaic systems are connected to the grid but there are still some few stand-alone installations, especially where there is no good grid coverage.

2.1.1 Model

The built in model from Matlab/Simulink of the PV array consists of parallel connected strings of modules, each string consisting of modules connected in series. Depending on the solar irradiance and the temperature the voltage-current curve changes as described by 2.1b this behaviour is modelled in Matlab/Simulink with a current source and diode circuit [4], presented in figure 2.1a.

2.1.2 Maximum Power-Point Tracking

The main drawback of PV systems may be its low efficiency, it is therefore imperative, moneywise, to extract as much of the energy available from the system. Changes in the environmental conditions affect the characteristics of the PV system, so the voltage (V_{MPP}) associated with the maximum power point (P_{MPP})

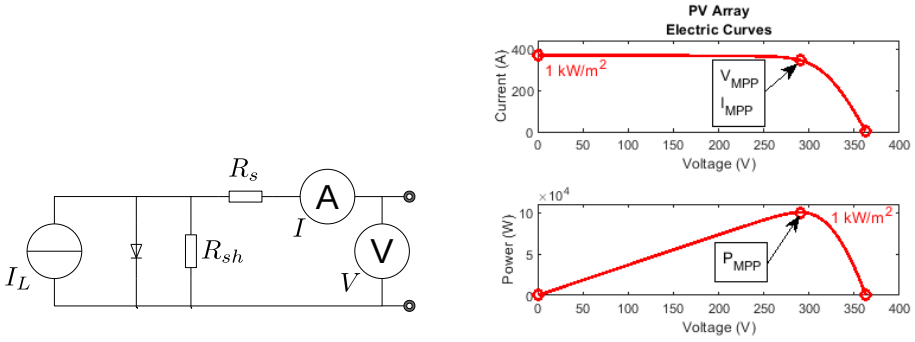

(a) **(b)**

Figure 2.1: (a) Internal representation of the PV modules in Matlab/Simulink, (b) Behaviour of the current and power of PV modules

also varies, figure 2.1b shows the power vs. voltage curve for a given irradiance and temperature, where this maximum point can be observed.

There are several methods to track the maximum power point, like the perturb and observe one which constantly changes the duty cycle of the interfacing converter looking for the direction where extracted power increases [5]. In this thesis another method, the incremental conductance one is used.

The incremental conductance method uses the voltage and current measurements from the PV system and the fact that the derivative of the power with respect to the voltage is zero at the MPP, as it can be observed in figure 2.1b. This means:

$$\frac{\delta(VI)}{\delta V} = I + V\,\frac{\delta I}{\delta V} \tag{2.1}$$

$$\left.\frac{\delta P}{\delta V}\right|_{MPP} = \left.\frac{\delta(VI)}{\delta V}\right|_{MPP} = 0 \tag{2.2}$$

$$\therefore \quad \left.\frac{\delta I}{\delta V}\right|_{MPP} = -\frac{I}{V} \tag{2.3}$$

The algorithm can be described with a flow chart as shown in figure 2.2. In this case the controlled variable is the voltage reference which is modified depending on the conditions of the voltage and current. In the flow chart the indexes k and k-1 are used to refer to the current measurement of the voltage or current and to the previous one, respectively. If certain conditions are met then the Reference voltage V_{ref} is increased, represented by (++), decreased (––), or maintained constant. This method has the advantage that it does not need to

oscillate around the maximum power-point to correctly track it, and is therefore preferred.

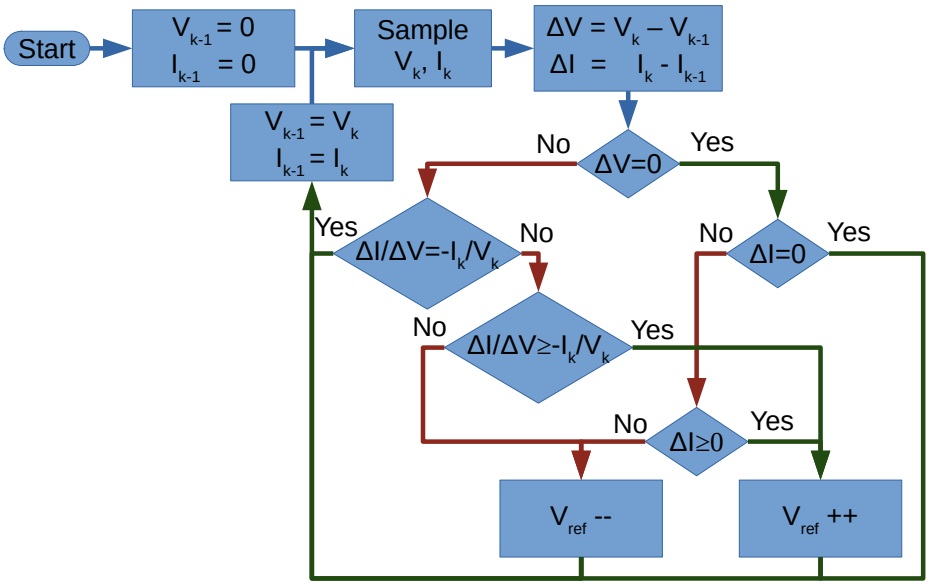

Figure 2.2: MPPT Flow chart based on voltage reference variation

2.1.3 Boost Converter

The MPPT algorithm presented above will provide the necessary voltage reference to achieve maximum efficiency, but an interface is still missing to allow for the voltage variations without affecting the stability of the DC bus. A DC-DC boost converter will perform this task. The duty cycle (δ) of the converter will be varied with a PI control to follow the voltage reference provided by the MPPT implementation. The variation of the duty cycle acts on the system by matching the source impedance with the load impedance [6], which is the necessary condition according to power flow theory to extract the maximum power from a generation device.

The topology of the boost converter is the one shown in figure 2.3. It has two main passive components, an inductor in the low voltage side, which reduces the current variations, and a capacitor in the high voltage side, which reduces the voltage variations. The diode ensures power will only flow from the low voltage side to the high voltage side, while the duty cycle of the switch is modified to control the voltage. By defining the maximum voltage and current variations desired and the parameters of the system it is possible to determine the values of the inductor (L) and capacitor (C). The design equations are:

$$L = \frac{V_{LV_{min}} \cdot (V_H V - V_{LV_{min}})}{f_s \cdot \Delta I \cdot V_H V} \tag{2.4}$$

$$C = \frac{I_H V \cdot (V_H V - V_{LV_{min}})}{f_s \cdot \Delta V \cdot V_H V} \tag{2.5}$$

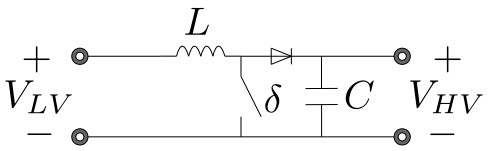

Figure 2.3: Circuit of a Boost converter

The relationship between the voltage and the duty cycle is given by the expression in equation 2.6, which assumes that the inductor current never reaches zero, this is known as Continuous Conduction Mode (CCM).

$$\delta = \frac{V_{HV} - V_{LV}}{V_{HV}} \tag{2.6}$$

$$\frac{V_{LV}}{V_{HV}} = 1 - \delta \tag{2.7}$$

2.1.4 Control

Thanks to the MPPT the system knows the reference voltage. Equation 2.7 shows that voltage in the low voltage side is proportional to the duty cycle, a PI controller is used to determine the duty cycle needed to follow the voltage reference .

2.2 Battery Energy Storage System

BES systems are developed to store electric charge to use it at a later time, thus regulating the power in a system or optimizing profits on energy markets by storing the energy during low demand periods and selling during peak hours. They are becoming increasingly common as complements of intermittent sources of energy like wind and solar power.

Compared to other Energy Storage Systems (ESS), batteries offer some clear advantages. They do not have geographical limitations like pumped hydro systems, and have a small footprint, depending on the technology used, BES systems also offer high power and energy densities with fast response times.

The battery system is usually represented with a constant voltage source with an internal resistance modelled with a series of parallel RC branches which provide different time constants. In this document the battery is simply modelled as a constant voltage source, so the charge and discharge dynamics as well as the effect of the state of charge are not considered.

2.2.1 Buck-Boost converter

Just like with the PV system, the BESS needs an interface to connect to the DC bus. Since in this application it will be used to regulate the power oscillations from the PV system, a converter that ensures that the DC voltage remains stable is needed. With the PV system a boost converter was used because the voltage from the PV system is smaller than the DC bus, and the power flow is always from the PV system to the DC bus. For the BESS, there will be situations where it will have to compensate for a lack of solar power and inject power, for which a boost converter is needed, but there will also be the need to absorb energy when the production is greater than the demand for which a buck converter is needed.

In this application it must be noted that the buck-boost converter is not the converter which can either increase or decrease the voltage level at the output, but rather send energy in both directions, from the high voltage side to the low voltage side with its buck operation and vice versa with its boost operation. In this sense the output of one system is the input of the other, and only one of the converters is active at a time.

The converter topology used can be seen in figure 2.4. With δ_1 it operates as a buck charging the battery on the low voltage side, and with δ_2 it operates as a boost injecting energy into the DC bus at the high voltage side. The design equations are the same as the ones mentioned in the boost converter for the PV system, these are also shared by the buck converter since the input and output are swapped.

$$\delta_1 = \frac{V_{LV}}{V_{HV}} \tag{2.8}$$

$$\frac{V_{HV}}{V_{LV}} = \frac{1}{\delta_1} \tag{2.9}$$

$$\delta_2 = \frac{V_{HV} - V_{LV}}{V_{HV}} \tag{2.10}$$

$$\frac{V_{HV}}{V_{LV}} = \frac{1}{1 - \delta_2} \tag{2.11}$$

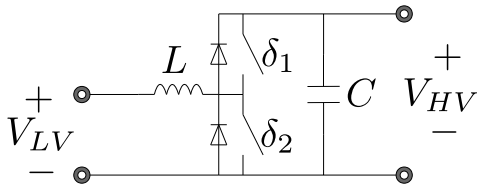

Figure 2.4: Circuit of a Buck-boost converter

2.2.2 Control

Equations 2.9 and 2.11 show the relation between the voltage and duty cycle for each operation mode assuming CCM. A PI compensator is again proposed to determine the duty cycle. Considering that only one mode should operate it would result inconvenient to use the voltage error as signal to determine the converter mode, so instead the current is used, which in CCM is more stable than the voltage.

2.3 Power Electronic Inverter

The inverter is the keystone in most modern power converters and is completely indispensable in the interconnection of DC microgrids with the grid. Inverters nowadays are fully controllable and can, with high precision, inject into or absorb power from the grid. Control methods allow to independently regulate, voltages, frequency, and active and reactive power making the inverter a flexible and fast component in the system.

The main disadvantage of inverters is that the oscillating behaviour is artificially achieved by electronic switching devices and therefore lacks the frequency stability that the inertia of large rotating machines provided. This problem is being addressed on two fronts, one is by the utilization of BESS as a source or sink of energy replacing the energy stored in the heavy rotors, and the second is by developing control techniques that better replicate the inertial response in these machines.

The basic model of a three phase inverter is the one shown in figure 2.5. There are several ways of controlling an inverter and there are other topologies that allow for more step variations, but for this thesis this simple model is used. The switches will be controlled with bipolar modulation technique which implies that when operating the device, the switches in a leg close in a complementary way, i.e. when S_a is open then S'_a is closed.

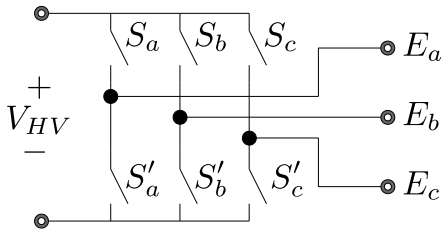

Figure 2.5: Circuit of a two-level inverter

2.3.1 Sinusoidal Pulse Width Modulation

For the inverter to produce an AC signal with low harmonic distortion that closely resembles that of a three phase generation device, the electronic switches have to be turned on and off appropriately. The PWM technique can provide the turn-on signals required, by controlling the duty cycle to output a signal whose moving average value for relatively short intervals is proportional to a reference value.

In the case of an inverter this reference value is a sinusoidal wave, this is known as Sinusoidal PWM or SPWM, where three sinusoidal signals, corresponding to the three phases, are compared to a high frequency triangular carrier, to produce the variable width pulses that drive the inverter.

By switching between on and off, conduction losses are minimized, and since the average of the signal is a sinusoidal wave the output will follow the same behaviour. In 2.6 a graphic description of the technique is presented, if the lower signal is filtered then a sinusoidal signal proportional to the modulating signal is obtained.

Assuming a carrier signal with amplitude from -1 to 1 and a modulating signal with maximum amplitude between this levels, then the sinusoidal signal obtained at the output of the inverter will have a peak amplitude of half the voltage of the DC bus by the ratio between the amplitude of the modulating signal and the carrier.

2.3.2 LCL Filter

The effect of the modulation will produce high order harmonics in the current so an LCL filter is connected at the output of the inverter in the AC side. The topology of an LCL filter is shown in figure 2.7, R_1 and L_1 are on the inverter side, and R_2 and L_2 are on the grid side. The components are tuned to correctly filter the switching frequency f_s (or angular frequency w_s) while having an adequate resonance frequency to provide the desired frequency response.

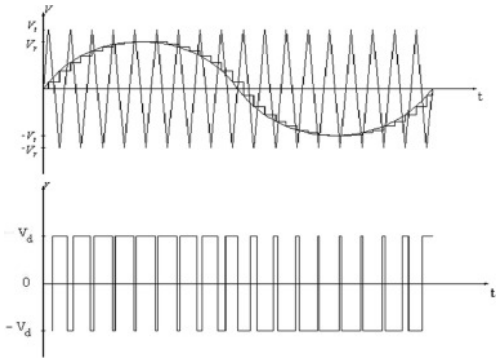

Figure 2.6: SPWM signal

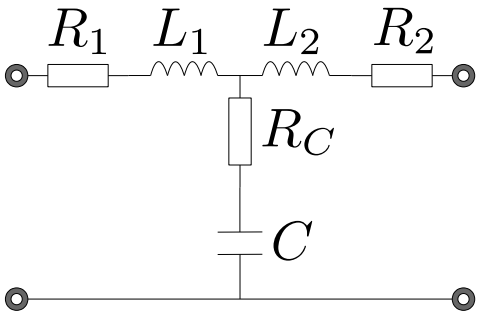

Figure 2.7: Circuit of an LCL filter

The capacitive component of the filter will produce a small amount of reactive power during the operation of the filter, it is usual to set this component to 5% of the base value. The design equations for the filter are as follows [7]:

$$L_1 = \frac{V_{DC}}{6 f_s \Delta I_L} \tag{2.12}$$

$$L_2 = \frac{\sqrt{\frac{1}{k_a^2}} + 1}{C \omega_s^2} \tag{2.13}$$

$$C = 5\% C_{base} \tag{2.14}$$

$$R_C = \frac{1}{3}\sqrt{\frac{L_1 L_2}{C(L_1 + L_2)}} \tag{2.15}$$

$$V_{DC} = \frac{2V_{AC}}{M}\sqrt{\frac{2}{3}} \tag{2.16}$$

To ensure that the filter will not present an undesirable behaviour around the resonance frequency, some conditions are required: the switching frequency should be at least twice as high, and the grid frequency at least a decade below. This is:

$$10 \cdot f_g \leq f_r \leq \frac{1}{2} \cdot f_s \tag{2.17}$$

Where f_g is the grid frequency, usually 50 or 60 Hz and f_r is the resonance frequency of the filter, which is calculated as follows:

$$f_r = \frac{1}{2\pi}\sqrt{\frac{L_1 + L_2}{L_1 L_2 C}} \tag{2.18}$$

2.3.3 Vector Controller

The generation of the signals needed for the SPWM method can be challenging as, by nature, an AC system is oscillating. Thanks to Park's transformation it is possible to model the inverter in a rotating reference frame, simplifying the study of the system and its control. With this control approach the measurements are transformed to the dq frame changing the alternating signals into constant values, modelling the system in this reference frame then allows to design a controller that generates the voltage references. By returning the references to the abc frame these can now be used on the modulator. With this control method the PI controllers used receive step signals as references, and not sinusoidal signals as with other methods. Figure 2.8 shows the steps followed when Park transformation is used within a control scheme.

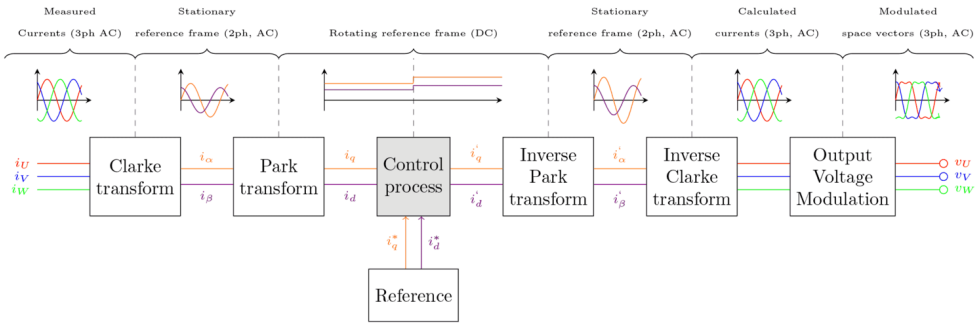

Figure 2.8: Vector Control scheme with dq transformation [8]

Park Transformation

This transformation consists in a mathematical manipulation of a three-phase signal such that the AC waveforms become DC signals in this new reference frame. It was initially used on the analysis of synchronous machines, aiding in simplifying their study and eliminating undesirable time-varying effects, allowing for the system to be treated as a linear time-invariant system. Nowadays it is very useful for the control of three-phase inverters as it simplifies their study and helps in decoupling certain electric parameters like active and reactive power, or AC and DC voltage magnitudes.

The transformation is usually represented in a matrix form, that by premultiplying the column vector of three-phase voltages returns the signals in the new reference. To perform the transformation, the value of the angle is needed, this is usually provided by a PLL or an integrator. The way this transformation is implemented in Simulink is such that the rotating frame is aligned 90 degrees behind the phase A; the matrix operations that describe it and its inverse transformation are:

$$\begin{bmatrix} u_d \\ u_q \\ u_0 \end{bmatrix} = \frac{2}{3} \begin{bmatrix} \sin\omega t & \sin\omega t - \frac{2\pi}{3} & \sin\omega t + \frac{2\pi}{3} \\ \cos\omega t & \cos\omega t - \frac{2\pi}{3} & \cos\omega t + \frac{2\pi}{3} \\ \frac{1}{2} & \frac{1}{2} & \frac{1}{2} \end{bmatrix} \begin{bmatrix} u_a \\ u_b \\ u_c \end{bmatrix} \tag{2.19}$$

$$\begin{bmatrix} u_a \\ u_b \\ u_c \end{bmatrix} = \begin{bmatrix} \sin\omega t & \cos\omega t & 1 \\ \sin\omega t - \frac{2\pi}{3} & \cos\omega t - \frac{2\pi}{3} & 1 \\ \sin\omega t + \frac{2\pi}{3} & \cos\omega t + \frac{2\pi}{3} & 1 \end{bmatrix} \begin{bmatrix} u_d \\ u_q \\ u_0 \end{bmatrix} \tag{2.20}$$

It will be assumed that the system is balanced and that the homopolar component (u_0) after the transformation is zero and can therefore be omitted, so in the following sections only components d and q will be mentioned.

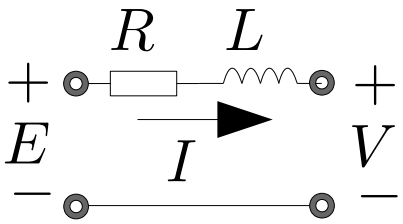

Figure 2.9: Circuit representation of a phase of the grid-tied system

Model

When an inverter is connected to a grid, situation which is referred to as Grid-tied, the inverter is modelled as a voltage AC source connected to another source through an inductive-resistive (RL) branch. This branch not only connects the system to the grid, but also serves as filter for the high-order components induced by the PWM. In this thesis, an LCL filter is proposed as the interfacing component but it can be considered just like an RL branch by taking the measurements before the second inductance, otherwise the dynamics of the capacitor would have to be included in the model. The circuit considered for this calculations is in figure 2.9. With Kirchhoff's voltage law the relation between the inverter's voltage and the current through the RL branch is obtained, and using Park's transformation it can be represented in the dq frame.

$$E = RI + L\frac{dI}{dt} + V \tag{2.21}$$

$$E_{dq} = RI_{dq} + L\frac{dI_{dq}}{dt} + L\omega\begin{bmatrix}0 & -1\\ 1 & 0\end{bmatrix}I_{dq} + V_{dq} \tag{2.22}$$

E, V and I are column vectors representing the components in abc reference, and E_{dq}, V_{dq} and I_{dq}, in the dq reference frame ignoring the homopolar component. E is the inverter's voltage, I is the current through the RL branch, V is the grid's voltage, and ω is the systems frequency.

$$E = \begin{bmatrix}e_a\\ e_b\\ e_c\end{bmatrix} \qquad E_{dq} = \begin{bmatrix}e_d\\ e_q\end{bmatrix}$$

$$V = \begin{bmatrix}v_a\\ v_b\\ v_c\end{bmatrix} \qquad V_{dq} = \begin{bmatrix}v_d\\ v_q\end{bmatrix}$$

$$I = \begin{bmatrix}i_a\\ i_b\\ i_c\end{bmatrix} \qquad I_{dq} = \begin{bmatrix}i_d\\ i_q\end{bmatrix}$$

The $L\omega$ term in the dq representation of the model comes from the result of Park's transformation of the derivative with respect to time of the current.

$$Park\left\{\frac{d}{dt}\begin{bmatrix} i_a \\ i_b \\ i_c \end{bmatrix}\right\} = \frac{d}{dt}\begin{bmatrix} i_d \\ i_q \end{bmatrix} + \omega\begin{bmatrix} -i_q \\ i_d \end{bmatrix} \tag{2.23}$$

The block diagram in Laplace domain of the grid-tied system with the inverter's voltage as input (E_{dq}) and the current as output (I_{dq}) can be represented with the voltage and current terms added before an LR branch, as seen in figure 2.10b

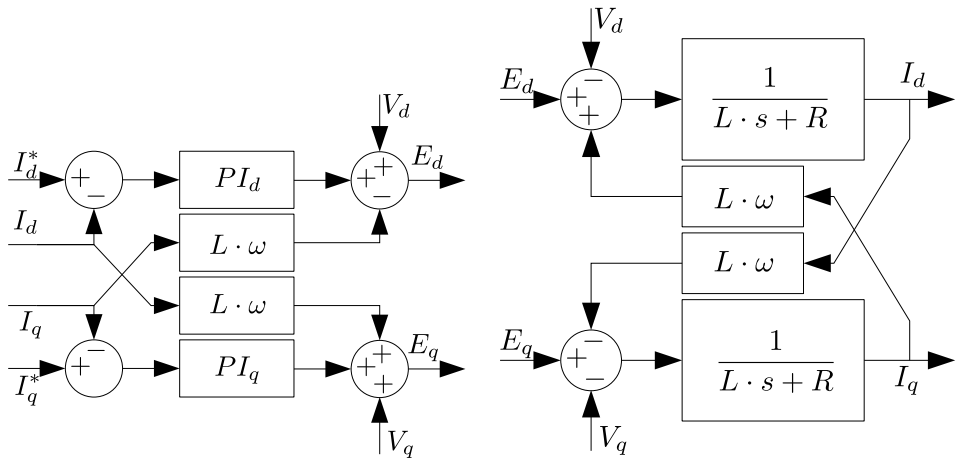

(a) **(b)**

Figure 2.10: (a) Block representation of the current controller, (b) block representation of the grid-tied system in dq frame

Current control

As it was seen above, the relations between the currents and the voltages in the dq frame have the grid voltage and the current components as disturbances. The advantage is that this are all measured values, readily available. To control the current components I_d and I_q independently a perturbation opposite to the one that the grid voltage and currents produce is added at the end of the controller to cancel the perturbation and the effect of the q component of the current in I_d, and vice versa. In figure 2.10a the current controller with a PI loop and this method is illustrated. By doing this not only are the currents decoupled, but the system becomes a simple loop with two blocks which makes the PI tuning process straightforward.

Current Limiter

Inverters as any other electronic device are rated for a certain current, so it is important to take it into consideration when designing the control. The references provided to the current controller have to be limited to avoid the total current from exceeding the limit. In the dq frame the total current is calculated by Pythagoras' theorem as $|I| = \sqrt{I_d^2 + I_q^2}$. It is usual that one of the components is allowed to take any value as long as its magnitude is less than the limit while the other component is limited by allowing it to be at most whatever magnitude is left before reaching the limit, this is $I_{q_{max}} = \sqrt{|I|_{max}^2 - I_d^2}$. It is possible to give priority to either the d or the q component depending on the application.

Power/ Voltage control

The current controller is at the core of the vector modulation, but setting the value of the current is rarely the main objective. Usually, defining the injected powers or the magnitude of the voltages is desired so an external control loop is designed to provide the current references for the current controller. Depending on the operation mode of the inverter it can either control the injected active and reactive power or the components of the voltage at the point of connection with the load.

In the dq frame active and reactive power are calculated as:

$$P = I_d \cdot V_d + I_q \cdot V_q \tag{2.24}$$
$$Q = I_d \cdot V_q - I_q \cdot V_d \tag{2.25}$$

When performing Park's transformation the angle is conveniently selected such that V is aligned with the d axis, making $V_q = 0$ leading to the following expressions:

$$P = I_d \cdot V_d \tag{2.26}$$
$$Q = -I_q \cdot V_d \tag{2.27}$$

When grid-tied, the voltage and frequency are fixed and variations in the current components affect proportionately the active and reactive power. As I_d increases P increases, and as I_q increases Q decreases. When disconnected from the grid and providing energy to a local load, the active and reactive power are fixed by the load and variations in the current components affect the components of the voltage. As I_d increases V_d increases and as I_q increases V_q increases. This represents a challenge as the control for the q component is inverted for one mode of operation, but it is easily solved by multiplying one of the error signals by -1.

Anti-Islanding Protection

It is considered dangerous to operate inverters inadvertently disconnected from the grid, i.e. operating in islanded mode while physically connected to the powered down grid. Because of this it is needed to detect such condition quickly and disconnect from the grid in short notice.

In [9] a proposal for an anti-islanding protection(AIP) for inverters is presented. The advantages of this implementation is that it uses values that are already available in the control, which are the power and voltage error signals. When one of the power references is not met for a given time, then the other power reference is modified, in this way even if the power injection was similar to the load the islanding condition can be detected. A delay is needed to ensure the system's compliance with fault ride-through requirements.

This implementation is thought for inverters that operate near the power factor, and can therefore identify the islanding condition by the discrepancy of the reactive power.

Operation Modes

There are two switches that control the connection of the inverter to the grid, one connects the inverter with the local loads and is used during both modes, and the other connects the inverter and local loads to the grid which is used during grid-connected mode.

If the grid switch (S_g) is closed, the inverter voltage has to first match the grid voltage to close the inverter's switch (S_i). In the other case when switch S_g is open, then matching the voltage at the PCC is needed before closing the switch.

2.4 Local Load & Grid

At the PCC there is a load connected that represents the load that is energized during the islanded mode of operation. This can be represented with a simple RL branch which will set an active and reactive power demand for the inverter. In figure 2.11 the circuit of one phase of the system from the inverter's output to the grid is presented. The local load is represented by L_l and R_l.

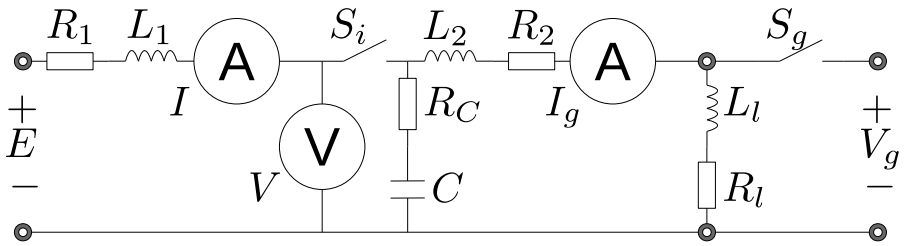

Figure 2.11: Circuit of one phase of the system with local load and grid connection

Chapter 3

Literature Review on Reconnection Methods

This chapter serves as a literature review on reconnection methods for microgrids. It aims to familiarize the reader with the current approaches, their achievements, advantages, and drawbacks. It is also intended to serve as a point of comparison when measuring the performance of the method presented in this report.

3.1 Controllable Variable Reactors

Y. Zhang, R. Dougal and H. Zheng proposed a reconnection technique that can be applied on microgrids in the absence of a communication network [10]. The problem in such networks is that even if the synchronization status is detected, two systems operating at almost the same frequency would take too long to synchronize on their own which is not permissible. To address this problem a controller of variable reactors is presented as a promising device to achieve a smooth reconnection between grids while reducing system oscillations.

The power between grids is calculated with classic power flow equation under the assumption of a purely inductive branch at the PCC.

$$p(\delta) = \frac{\left|V_{mg}\right| \cdot \left|V_{g}\right|}{X_{tieline} + X_{VR}(t)} \sin\delta \tag{3.1}$$

The value of the variable reactance is controlled to minimize the initial power flow following the reconnection. The control procedure consists on maintaining the highest reactance value, which is defined by specifying a threshold current, for a certain period of time, after this period if the current is below the threshold then the reactance is gradually reduced until it reaches its minimum

value and the connection is considered complete.

$$X_{max} \geq \frac{\left|V_{mg}\right| + \left|V_{g}\right|}{I_{th}} \tag{3.2}$$

The results obtained with this method between two 47 MVA microgrids demonstrate a reduction in the current peak value ending up in approximately 10% of what was observed without the reactor. In the same way, voltage and frequency variations were greatly reduced as well.

The tuning of this device is very important as a holding period which is too long or too short has detrimental effects in the oscillations and its duration. It presents itself as a cheap solution which can dispense of a communication system but that does not work seamlessly.

3.2 Dispatch Unit at the PCC

T. Uten, C. Charoenlarpnopparut and P. Suksompong provide a radically different approach to the reconnection problem [11]. An additional Distributed Generator (DG) referred to as the Dispatch Unit (DU) is installed at the PCC and is controlled to generate the necessary power to adjust the electric parameters with those of the grid. The distributed generators in the microgrid operate with a droop control, the frequency and voltage command is set depending on the power calculation.

For the DU, the droop controller uses the microgrid's frequency and the angle error along with the power calculation to determine the angle and voltage commands. A separate logic monitors the voltage, frequency and angle difference until the reconnection conditions are met and the switch is closed.

With this implementation, synchronization times of less than 5 seconds were achieved, it was also noted that the size of the DU need not be larger than 2.5% of the aggregate capacity of the microgrid. The control proposed is very efficient and can obtain near seamless reconnections without the need of a communication system.

An important insight from this paper is that even though reconnections are allowed with phase differences of up to 10^o, the reconnection is really only seamless when the difference is less than 1^o [11].

3.3 Communication-based cooperative control

Other authors like C. Cho [12] and D. Shi [13] propose methods that achieve the synchronization by controlling all variable DGs to set the frequency and voltage of the microgrid while renewable DGs operate at their maximum efficiency.

In [12], the control is achieved by sending offset signals to each DG in order to have all of them aid in the reconnection process proportionately. The technique was tested with some renewable sources, two Diesel Engines as DGs and a BESS. The generators would be commanded to modify their power injection to adjust the frequency and phase while the BESS would compensate by absorbing the extra power injected in the system.

Their result was that in less than 6 seconds the system was able to successfully synchronize but not without some observable power oscillations. It was noted that the communication delay was of utmost importance, as too long delays led to system instability.

While in the proposal of [12] all systems receive simultaneously the commands through the same communication bus, in [13] an Ethernet connection is used, the signals are sent to one of the DGs and from it it forks and is sent to the others. Instead of sending individual commands to each, they all receive the same references and they distribute the load evenly by means of droop coefficients chosen based on the DG capacities.

The references are set by a central controller with a PI compensator, so despite the DGs operating with droop controllers the electric parameter differences between the grid and the microgrid can be eliminated before reconnecting the systems.

The results under ideal conditions are very promising, the system is able to synchronize in about 5 seconds and the load is correctly distributed on all 4 DGs used during the simulation. Even in the presence of communication delays the system is able to synchronize flawlessly. The only factor that was observed to affect the speed of the synchronization was the inertia of the DGs, but the system remained stable.

3.4 Virtual Current on Universal Droop Controller

M. Amin [14] proposed for inverter-based distributed generators controlled with the Universal Droop Control (UDC) to add to the current measurement, a value which is proportional to the current that would flow between the grid and

microgrid through a virtual branch, since this current is not really there, the system will adjust the voltage and frequency to minimize this virtual current, therefore eliminating the error between at the PCC, allowing for a smooth reconnection.

The UDC was originally proposed in [15, 16] and has the advantage of providing an efficient droop-based control that can work with any type of inverter, it also allows for the operation in parallel of inverters with different impedances. Thanks to the modification made in [17] it is able to to follow power set-points and synchronize itself to start operating connected to the grid.

A similar implementation to the one used to self-synchronize is used to resynchronize when changing from islanded mode to grid-connected mode.

Since this procedure is proposed for an inverter, it is able to achieve the synchronization criteria very quickly, in less than a second.

The advantages of this technique are that it does not require a communication network or a frequency measuring device like a PLL, and is yet able to seamlessly synchronize with the grid.

Chapter 4

Structure of the Microgrid

This chapter introduces the microgrid model used to test the proposed implementation. The system parameters are defined, and the design of each element is shown and justified.

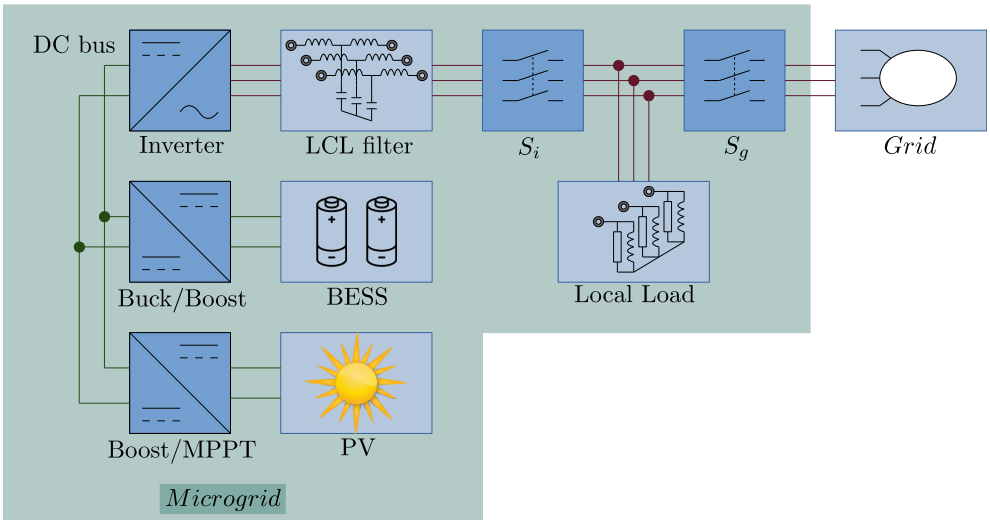

Figure 4.1: Microgrid block model

4.1 Photovoltaic System

The Photovoltac (PV) system proposed consists of an array of solar panels which can provide 100 kW of Power at a voltage around 300 V. The voltage is controlled with a boost converter with an MPPT control based on the variable admitance method. Being in this way able to extract the highest amount of energy from the sun without inserting much oscillations into the system. The converter is designed and dimensioned considering the 100 kW rating of the solar array.

There can be nonetheless undesirable power fluctuations when the irradiance of the sun or the temperature change.

4.1.1 Array

For the solar array, a model equivalent to 47 parallel strings of 10 series-connected modules each is used based on the model presented in figure 2.1a in page 8. The I-V and P-V curves of this array is shown in figure 4.2 for different irradiances at a constant temperature and in figure 4.3 for different temperatures at a constant irradiance.

4.1.2 Boost Converter

The output of the array is connected to a boost converter. The output voltage of the converter is the DC bus voltage which is assumed to be constant at 800 V. The input which is variable depends on the PV system, based on the curves presented in figure 4.2 and figure 4.3, the range is set between 250 V to 400 V. Its power capabilities is the same as that of the array, 100 kW. The switching frequency is arbitrarily set to 5 kHz, the maximum current variation in the inductor is considered to be 5% and the output voltage variation of 1%.

Using the design equation previously studied in chapter 2 and from the specifications from the previous paragraph all the necessary values can be obtained or calculated.

$$
\begin{aligned}
I_{LV_{max}} = \frac{P}{V_{LV_{min}}} = \frac{100kW}{250V} &= 400A \\
I_{HV} = \frac{P}{V_{HV}} = \frac{100kW}{800V} &= 125A \\
\Delta I = 5\% I_{LV_{max}} &= 20A \\
\Delta V = 1\% V_{HV} &= 8V
\end{aligned}
$$

The components of the converter can then be determined:

$$
\begin{aligned}
L = \frac{V_{LV_{min}} \cdot (V_{HV} - V_{LV_{min}})}{f_s \cdot \Delta I \cdot V_{HV}} = \frac{250V \cdot (800V - 250V)}{5000Hz \cdot 20A \cdot 800V} &= 1.72mH \\
C = \frac{I_{HV} \cdot (V_{HV} - V_{LV_{min}})}{f_s \cdot \Delta V \cdot V_{HV}} = \frac{125A \cdot (800V - 250V)}{5000Hz \cdot 8V \cdot 800V} &= 2.1mF
\end{aligned}
$$

Maximum Power Point Tracking algorithm

To control the boost converter the duty cycle will be determined with an MPPT method known as the incremental conductance algorithm. From the specifications and numerical results presented above the range of operation of the system is already known, so the algorithm can be easily implemented in Matlab having the

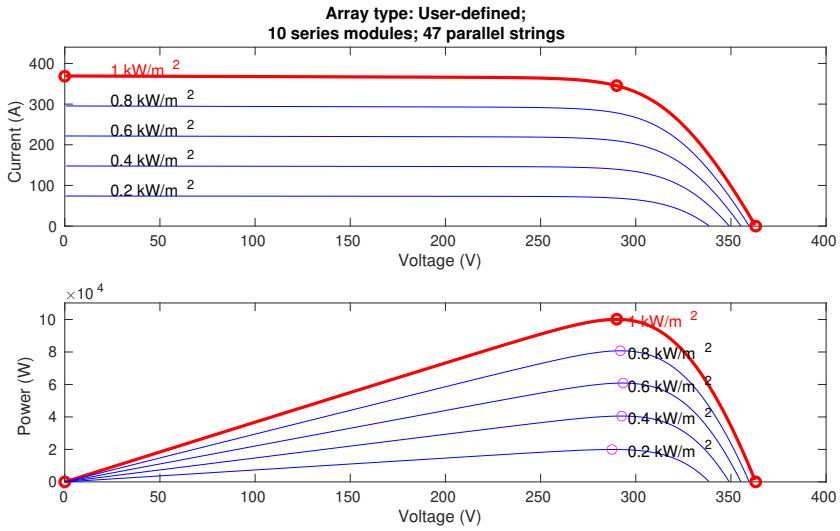

Figure 4.2: Current-Voltage and Power-Voltage curves at constant temperature

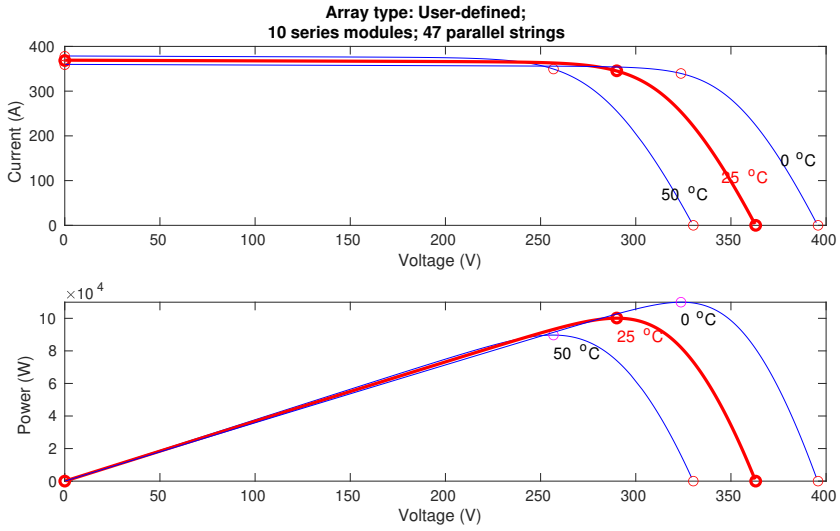

Figure 4.3: Current-Voltage and Power-Voltage curves at constant irradiance

voltage and current of the solar array as inputs and providing a voltage reference as output.

Code listing 4.1: Implementation of the Incremental Conductance MPPT method

```
function Vref = RefGen(V, I)

Vrefmax =   400;
Vrefmin =   250;
Vrefinit =  290;
deltaVref = 0.005;
persistent Vold Iold Vrefold;

dataType = 'double';

if isempty(Vold)
    Vold =  0;
    Iold =  0;
    Vrefold = Vrefinit;
end

dV =        V-Vold;
dI =        I-Iold;

if dV == 0
    if dI == 0
        Vref = Vrefold;
    elseif dI > 0
        Vref = Vrefold + deltaVref;
    else
        Vref = Vrefold - deltaVref;
    end
elseif dI/dV == -I/V
    Vref = Vrefold;
elseif dI/dV > -I/V
    Vref = Vrefold + deltaVref;
else
    Vref = Vrefold - deltaVref;
end

if Vref >= Vrefmax || Vref <= Vrefmin
    Vref = Vrefold;
end

Vrefold = Vref;
Vold = V;
Iold = I;
```

4.2 Battery Energy Storage System

To address the power oscillations from the PV system a battery energy storage system (BESS) controlled with a buck and boost converter is used to absorb or provide the necessary energy. The converter is dimensioned with the same rating as that of the PV system but realistically it would not need be that high. For the battery a 300 V source is selected.

4.2.1 Buck-Boost Converter

To connect the battery to the DC bus an interface is needed due to the voltage difference. A buck-boost converter is used as interface, which allows the battery to absorb energy during buck operation and inject energy during boost operation, depending on what is needed. The switching frequency is set at 5 kHz, and the other parameters are as specified in the Solar array section above.

$$\begin{aligned} I_{LV} &= \frac{P}{V_{LV}} = \frac{100kW}{300V} && = 333.3A \\ I_{HV} &= \frac{P}{V_{HV}} = \frac{100kW}{800V} && = 125A \\ \Delta I &= 5\% I_{LV} && = 16.7A \\ \Delta V &= 1\% V_{HV} && = 8V \end{aligned}$$

The inductor needed for this converter is the following one.

$$L = \frac{V_{LV} \cdot (V_H V - V_{LV})}{f_s \cdot \Delta I \cdot V_H V} = \frac{300V \cdot (800V - 300V)}{5000Hz \cdot 16.7A \cdot 800V} = 2.25mH \quad (4.1)$$

$$C = \frac{I_{HV} \cdot (V_{HV} - V_{LV_{min}})}{f_s \cdot \Delta V \cdot V_{HV}} = \frac{125A \cdot (800V - 300V)}{5000Hz \cdot 8V \cdot 800V} = 1.95mF \quad (4.2)$$

Converter control

A PI compensator is used to determine the duty cycle for the switches, where the control variable is the DC bus voltage. The direction of the current is used to determine whether to inject or absorb energy.

4.3 Inverter

A standard three-phase inverter is proposed, controlled with the vector control, also known as dq decoupled control technique. The control is implemented on the components of the current which are set depending on the operation mode. During islanded mode the d component of the current is set to regulate the d component of the voltage at the PCC, and the q component of the current is set to make the q component of the voltage to zero, which is the necessary condition for the technique to work by decoupling the effects of the current components on the active and reactive power.

During grid-connected mode the d component is used to control the active power and the q component to maintain the reactive power at zero, i.e. unitary power factor. The proposed circuit is a standard three-phase inverter with three legs operated with bipolar modulation.

4.3.1 Filter

The effect of the modulation will produce high order harmonics in the current so an LCL filter is connected at the output of the inverter in the AC side.

The capacitive component of the filter will produce a small amount of reactive power during the operation of the filter, it is usual to set this component to 5% of the base value.

The switching frequency of the inverter is set to 10 kHz, the power rating is the same as for the photovoltaic system of 100 kVA, the attenuation factor k_a is chosen to be of 0.2, the current variation is limited to 10% of its maximum value, the DC voltage is already set to 800 V and the AC grid is set at 400 V.

$$P = 100kVA \qquad V_{DC} = 800V$$
$$V_{AC} = 400V \qquad f_s = 10kHz$$
$$k_a = 0.2 \qquad \Delta I = 10\%I_{max}$$

Using the design equations from [7] and the parameters defined above, the elements of the LCL filter can be determined.

$$Z_b = \frac{V_{AC}^2}{P} = 1.6\Omega$$
$$C_b = \frac{1}{\omega_g Z_b} = 1.989mF$$
$$I_{max} = \sqrt{\frac{2}{3}}\frac{P}{V_{AC}} = 204A$$
$$\Delta I = 0.1I_{max} = 20.4A$$
$$C_f = 5\%C_b = 99.5\mu F$$
$$L_1 = \frac{V_{DC}}{6f_s\Delta I_L} = 653\mu H$$
$$L_2 = \frac{\sqrt{\frac{1}{k_a^2}}+1}{C_f\omega_s^2} = 15.27\mu H$$
$$R_f = \frac{1}{3}\sqrt{\frac{L_1L_2}{C_f(L_1+L_2)}} = 129m\Omega$$
$$M = \frac{2V_{AC}}{V_{DC}}\sqrt{\frac{2}{3}} = 0.817$$

The resonant frequency is calculated to ensure it is far away enough from the relevant frequencies of the system, the switching frequency should be at least twice as high, and the grid frequency at least a decade below.

$$f_r = \frac{1}{2\pi}\sqrt{\frac{L_1 + L_2}{L_1 L_2 C_f}} \qquad = 4.13kHz \tag{4.3}$$

The resonance frequency calculated in equation 4.3 is clearly in the acceptable range, so the filter should not negatively impact the operation of the system at either the grid frequency or the switching frequency.

Chapter 5

Inverter Control

This chapter presents the tuning and control of the inverter. The control blocks are explained in detailed along with the tuning procedure and defined parameters. The structure of each control loop is studied and an overview of the operation modes of the microgrid is presented. In this chapter the necessary modifications needed to use the RSL as a synchronization block are presented.

In order to implement the vector control the angle of the voltage is needed. In this way the components can be aligned with the d axis when using Park's transformation, and follow the control procedure described in chapter 2. This is usually achieved with a PLL, which is known for being inconvenient and hard to control and tune. Droop control is usually seen as an alternative control scheme as it can dispense from the PLL with the drawback of not working at the nominal values. So before presenting the blocks used for the the vector control, the robust synchronization loop (RSL) will be introduced as the selected alternative to a PLL.

5.1 The Robust Synchronization Loop

The RSL will be explained in this section, an overview of its structure and tuning procedure will be given as well as the modifications needed on the original block proposed in [18] in order to not only use it as a PLL but also take advantage of its inherent control mechanism to easily synchronize to a grid.

5.1.1 Principle of operation

In the steady state, the RSL works as a PLL, It receives a three-phase signal as input, and outputs the frequency of this signal and its angle. What is special about the RSL is its transient response. The process it goes through to output the frequency measurement causes alterations in the frequency that gradually and precisely drive the system to the same frequency and phase. This is, if the input signal is the grid voltage and the system is lagging behind the grid, even if both are at the same frequency, the RSL will send a higher frequency signal for some

time and then will return to output the correct frequency. As a PLL this would be an undesirable behaviour, but as a synchronizer it is thanks to this behaviour that the lagging system accelerates and catches up with the grid seamlessly.

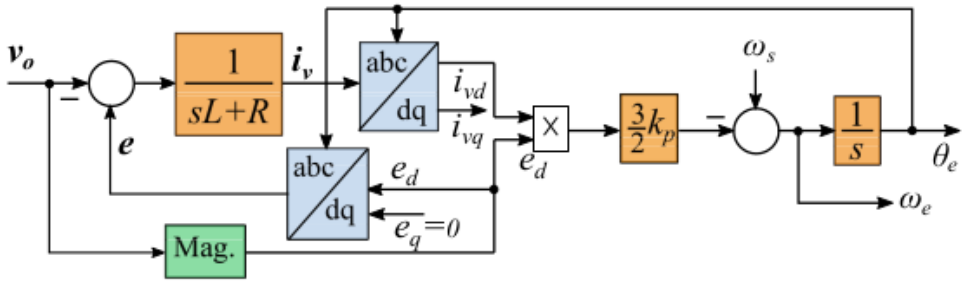

Figure 5.1: RSL model as presented in [18]

The way the RSL measures the grid's conditions is by estimating an internal voltage reference and calculating the power injection that would exist between this reference and the input voltage. This is achieved by using a virtual RL branch and using the virtual current and the reference voltage to calculate the power. This power is then scaled with a droop coefficient which is added to the nominal angular frequency. The angle obtained from integrating the result and the magnitude of the input voltage are used for the internal reference. The frequency deviation produced by the power calculation will bring the value of the output frequency to the same as the input frequency with a steady-state error in the output angle proportional to the difference of the frequency with respect to its nominal value. Figure 5.1 shows the block diagram of the RSL as proposed in [18].

5.1.2 Setup and tuning

As it was described above, the RSL works by calculating a virtual current, which produces a virtual power and a frequency variation proportional to it. The parameters needed for the RSL block are:

f_n	—	Nominal Frequency
R_v	—	Virtual Resistance
L_v	—	Virtual Inductance
Δf_v	—	Maximum virtual frequency variation
Δf_o	—	Maximum output frequency variation

Remembering that one of the limitations of the RSL is that there needs to be a phase error to accurately measure frequencies other than the nominal one, it is helpful to allow for the frequency variations to be relatively high in order

to minimize this error. To exemplify this: if the maximum frequency variation allowed were of 0.5 Hz this would mean that the phase error in steady state needed to measure a grid at 50.5 Hz would be of 90^o, whereas if the maximum variation were 5 Hz for the same 50.5 Hz grid the error would now be 5.74^o. Considering this, it is convenient to allow high frequency variations to ensure small errors, but at the same time this high frequency variations are undesirable for the system.

To overcome this problem two limits are set, one is the maximum virtual frequency variation Δf_v which sets the droop value and reduces the steady state error of the phase for off-nominal frequencies, and the second one is the maximum output frequency variation Δf_o which limits the output signal to a much narrower value.

5.1.3 Modifications to enable grid synchronization

From the original RSL block some modifications were made for it to work in the grid-connected mode, as well as in islanded mode, where it should provide a constant frequency reference.

For it to provide a constant reference during islanded mode, a switch is connected after the droop constant, so that the system only tracks the grid voltage when it is connected or in the process of synchronizing. A selector was also added for the droop constant such that smaller errors are obtained when synchronizing by having a larger maximum variation.

$$\text{High K:} \quad 8 * \pi^2 * f_n * L_v * \Delta f_v / 3 \tag{5.1}$$

$$\text{Low K:} \quad 8 * \pi^2 * f_n * L_v * 0.5 / 3 \tag{5.2}$$

The voltage magnitude is included in the output signals in order to match the microgrid's voltage magnitude during the reconnection and a synchronization signal is generated with the error of the frequency to indicate to the inverter when the synchronization process is completed. An additional parameter is considered for the RSL model to specify the error tolerance, which according to the regulations has to be smaller than 0.1 Hz. The Simulink model of the modified RSL is shown in figure 5.2

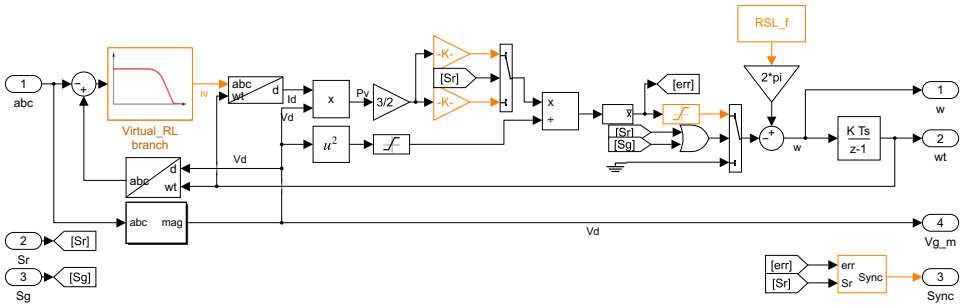

Figure 5.2: Simulink RSL model

5.2 Vector Control

The inner-loop of the control is for the current. It determines the inverter voltage which tracks the current references given, it is implemented with a PI compensator. This inner loop is common to all modes of operation. The outer-loop is also designed with a PI control but the reference is now a voltage or power and the output is the current reference for the inner-loop.

For the d loop, the inner-loop controls the d component of the current and the outer-loop controls either the Active Power or the d component of the voltage at the point of common coupling (PCC). The Voltage reference depends on whether the system is setting the voltage itself, e.g. to the nominal value, or tracking the grid to achieve resynchronization. For the q loop, the inner-loop controls the q component of the current while the outer-loop controls again either the q component of the voltage to 0, or the reactive power to zero.

5.2.1 Current Control

From the current reference up to the measured current the transfer function is composed of basically two blocks. Thanks to the decoupling and perturbation cancellation the terms involving the voltage and the other current component cancel out. The open loop transfer function is as follows:

$$H(s) = \frac{K_{pi}s + K_{ii}}{s} \cdot \frac{1}{Ls + R} \tag{5.3}$$

By using the simple approach of pole cancellation the coefficients can be selected to be the same as the values of the inductance and resistance multiplied by a gain K. By specifying then the crossover frequency a decade lower than the switching frequency of 10 kHz the PI parameters can be calculated.

$$H(s) = \frac{K}{s} \tag{5.4}$$

$$|H(jw)| = \left|\frac{K}{jw}\right| = \left|\frac{-jK}{w}\right| = 1 \tag{5.5}$$

$$K = w = 2\pi f \qquad = 6283 \tag{5.6}$$

$$K_{pi} = Lw \qquad = 8.168 \tag{5.7}$$

$$K_{ii} = Rw \qquad = 128.8 \tag{5.8}$$

This results in a controller with a response time of 1 ms. With the aid of Simulink PID Controller Tuning a robust 1 ms controller was defined with parameters in the same order as the ones here observed.

$$K_{pi} = 3 \tag{5.9}$$

$$K_{ii} = 90 \tag{5.10}$$

$$C_i(s) = \frac{3s + 90}{s} \tag{5.11}$$

5.2.2 Power Control

During the grid connected mode, the power is controlled in the outer loop, during this operation the voltage is set by the grid and can be considered constant so the block involving the term $\frac{3}{2}V_d$ can be modelled as a gain. By specifying the crossover frequency a decade below the current controller it is possible to consider the current controller to be a gain of 1 since it would be much faster. The active power grows in the same direction as the current, but the reactive power is the opposite way, so its controller has the same PI parameters but with the opposite sign. The open loop transfer function is:

$$H(s) = \frac{K_{pp}s + K_{ip}}{s} \cdot \frac{3}{2}V_d \tag{5.12}$$

To ensure stability a phase margin of 60^o or more is desirable

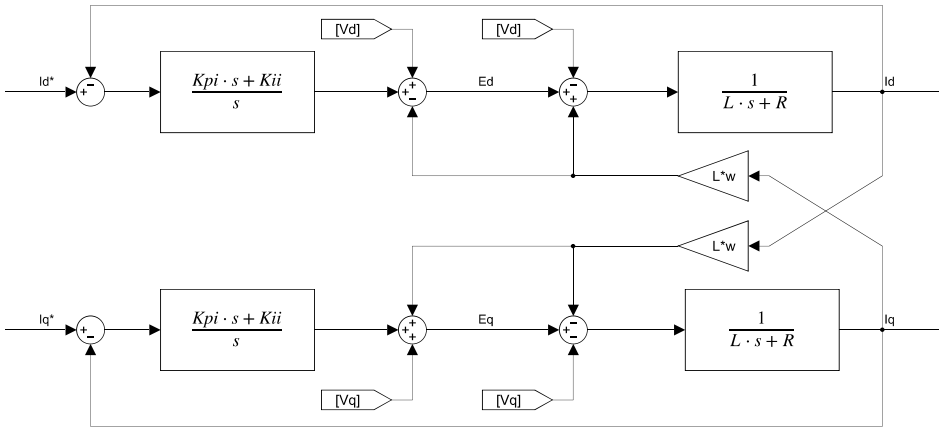

(a)

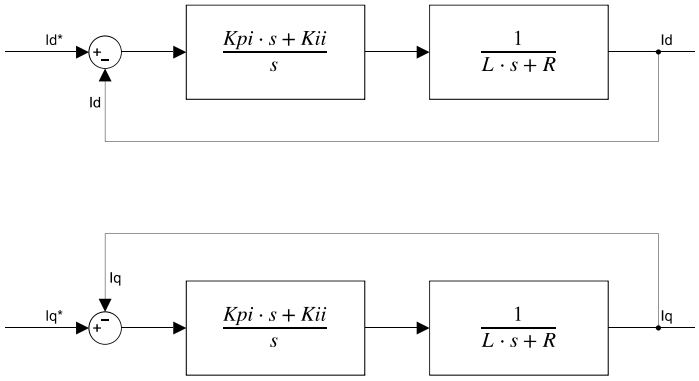

(b)

Figure 5.3: (a) Current control loop, (b) Simplified current control loop

$$V_d = 400\sqrt{\frac{2}{3}}$$

$$H_P(j\omega) = \frac{3}{2}V_d\frac{j\omega K_{pp} + K_{ip}}{jw} \tag{5.13}$$

$$|H_P(j\omega)| = \frac{3}{2}V_d\left|\frac{\omega K_{pp} - jK_{ip}}{\omega}\right| = 1 \tag{5.14}$$

$$\omega^2 = \frac{9}{4}V_d^2(K_{pp}^2\omega^2 + K_{ip}^2) \tag{5.15}$$

$$arg(H_P(jw)) = 60^o = \tan^{-1}(\frac{K_{ip}}{K_{pp}\omega}) + 180^o \tag{5.16}$$

$$\tan^{-1}(\frac{K_{ip}}{K_{pp}\omega}) = -120^o \tag{5.17}$$

$$\frac{K_{ip}}{K_{pp}\omega} = 1.7321 \tag{5.18}$$

Substituting 5.18 in 5.15

$$\omega^2 = \frac{9}{4}V_d^2(K_{pp}^2\omega^2 + (1.7321^2K_{pp}^2\omega^2) \tag{5.19}$$

$$K_{pp} = \frac{2}{3}\frac{1}{V_d\sqrt{1+1.7321^2}} \tag{5.20}$$

$$K_{pp} = 0.001 \tag{5.21}$$

$$K_{ip} = 1.111 \tag{5.22}$$

This controller worked correctly during normal operation but during a lost grid contingency was too fast and even though the system was stable it was not possible to detect the unintentional islanding due to the oscillations produced by the controller. With the aid of Simulink a robust controller with 50 ms response time was defined, as opposed to the 10 ms original design.

$$K_{pp} = 30 \cdot 10^{-6} \tag{5.23}$$

$$K_{ip} = 0.08 \tag{5.24}$$

$$C_P(s) = \frac{30 \cdot 10^{-6}s + 0.08}{s} \tag{5.25}$$

5.2.3 Voltage Control

During the islanded operation the voltage is no longer set by the grid and is now determined by the load. The current from the inverter now flows through the load and sets a voltage at the PCC, the model of the load in the dq frame involves

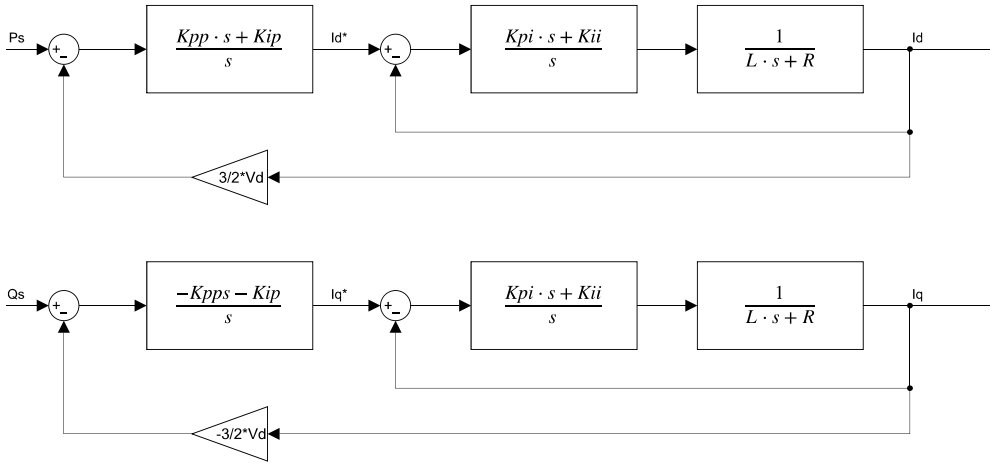

(a)

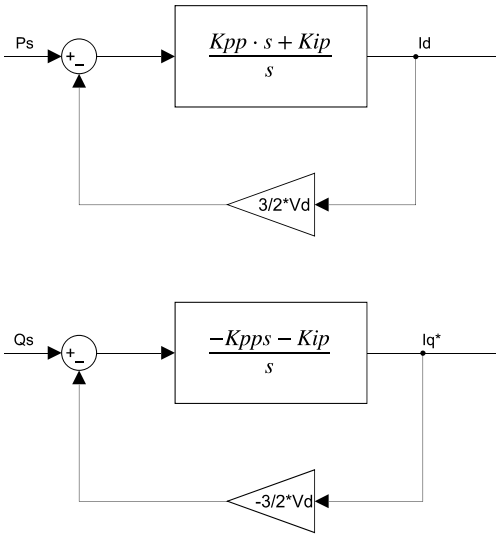

(b)

Figure 5.4: (a) Power control loop, (b) Simplified power control loop

an equivalent RL branch which represents the load and a perturbance involving the other current component. The voltage at the PCC in terms of the load and the inverter current is as follows:

$$V_d = I_d(sL_l + R_l) - L_l \omega I_q \tag{5.26}$$
$$V_q = I_q(sL_l + R_l) + L_l \omega I_d \tag{5.27}$$
$$\tag{5.28}$$

With the help of Simulink the following controller is designed with the same response time as the power control.

$$K_{pv} = 60 \cdot 10^{-6} \tag{5.29}$$
$$K_{iv} = 12 \tag{5.30}$$
$$C_v(s) = \frac{60 \cdot 10^{-6} s + 12}{s} \tag{5.31}$$

5.2.4 Outer Loop Soft Transition

The power control and the voltage control act on the outer loop of the control and are mutually exclusive, in order to avoid abrupt changes in the current references the same PI can be used for both controls. It can be observed that the K_i parameter is 150 times larger for the Voltage control so the voltage error is multiplied by this factor to compensate for that fact and at the output of the PI the error by a factor of $29.6 \cdot 10^{-6}$ is subtracted to return the K_p parameter to the right value.

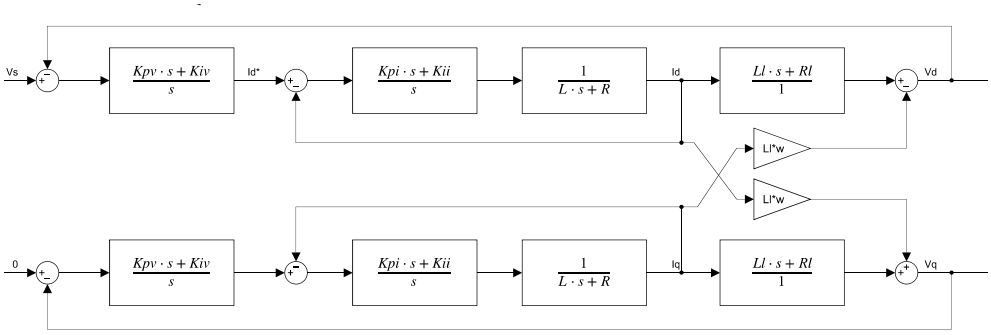

(a)

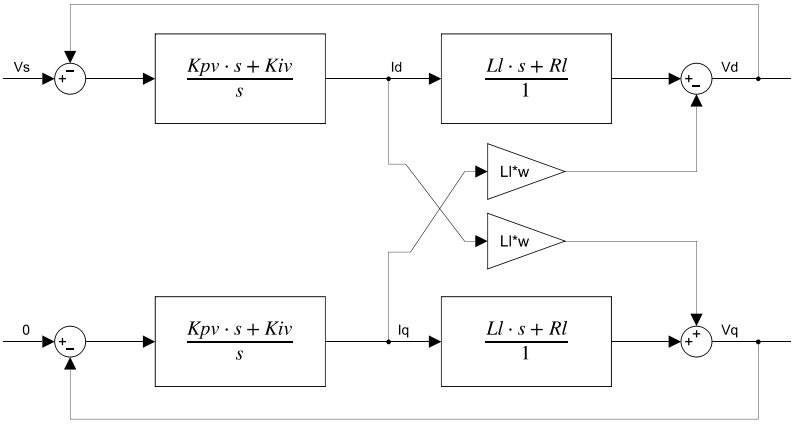

(b)

Figure 5.5: (a) Voltage control loop, (b) Simplified voltage control loop

5.3 Operation cases

With the control elements described in this chapter and the elements described for the AC system in chapter 2, the signals, switch conditions, and references for each operation mode will be presented in this section. It is possible to control from the grid the two switches, the switch that connects the inverter to the system (S_i), and the switch that connects the grid to the system (S_g).

On the controller it is possible to set the references of the outer-loop control, for the d-loop, the error signal (PI_d) can be either the active power error, the voltage error to a set-point or the voltage error to the grid voltage; for the q-loop, the error signal (PI_q) can be the reactive power error or the q component of the voltage error. Finally the other controllable features are the synchronization signal (S_r), used to trigger the resynchronization mechanism of the RSL, and the enable signal of the PWM generator (PWM) that controls the inverter gates.

Figure 5.6 shows the signals and references for each of the operation cases, in this chart dV, dP, and dQ are the voltage error, active power error, and reactive power error respectively. The voltage error depends on the S_r signal, being with respect to a set-point when off, and with respect to the grid when on. Figure 5.7 expands on the grid-connected behaviour including the states used for the unintentional islanded case.

5.3.1 Off

Normal

During this mode the inverter is disconnected from the system and the PWM generator is disabled. The error signals sent are kept at zero to disable the PI action. The grid switch can be in any position, since the local load can be energized by the grid while the inverter is disabled.

Start to islanded

To start the inverter in stand-alone mode the inverter switch is closed, the PWM enabled and the voltage control is selected. The inverter will quickly set the voltage and energize the local load.

Start to grid-connected

If it is the case that the grid is already feeding the local load, then the voltage generated by the inverter has to be matched to the one of the load. This is automatically achieved because of the structure of the current control that adds the voltage dq components after the PI compensator. To start its operation then only the alignment of the voltage with the d axis is needed, so the S_r signal is activated

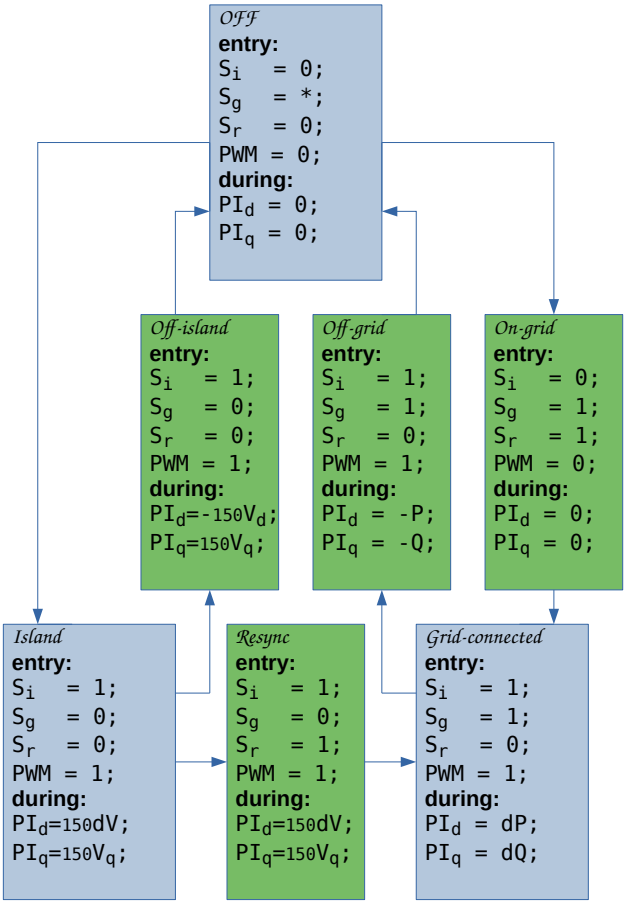

Figure 5.6: Chart representation of operation cases and their transitions

and the inverter waits for the synchronization signal to turn on the device and start controlling the power.

The RSL is on with large frequency variation droop constant, it provides the necessary frequency variation to align the internal voltage reference for the initial connection.

5.3.2 Islanded

Normal

During the islanded operation the voltage components are controlled, such that they remain aligned with the d axis and with the magnitude of the defined set-point. The grid switch is open in this mode and the RSL is off, which means it outputs a constant frequency signal.

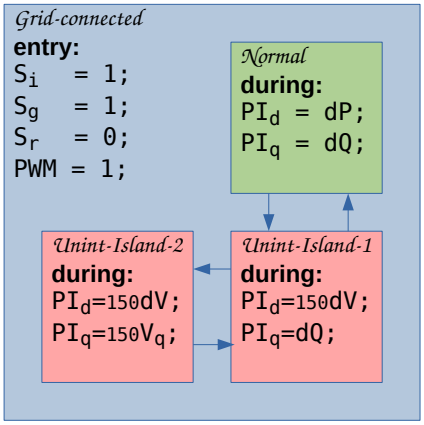

Figure 5.7: Chart of the grid-connected mode

The references of the outerloop are the voltage magnitude reference on d loop with d component of the voltage on the feedback, and zero value reference on the q loop with q component of the PCC voltage on the feedback.

The RSL is off, i.e. its input disconnected and constant frequency reference at the output.

Resynching

When the system is islanded and the grid is present a signal can be sent (S_r) to indicate the start of the resynchronization process. When this is received then the voltage reference is changed from the set-point to the measured value from the PCC and the RSL is allowed to modify the frequency in order to achieve the resynchronization. It internally is generating a reference voltage aligned with the d component while externally the system is controlling also the voltage components to align with the d component. When the RSL signals it has finished measuring the frequency the microgird will have resynchronized with the grid as well. During this transient the inverter is still controlling as it does during islanded mode.

The references of the outerloop are the grid voltage magnitude reference on d loop with d component of the voltage on the feedback, and zero value reference on the q loop with q component of the PCC voltage on the feedback.

The RSL is on in its grid frequency tracking mode during its transient period, i.e. during resynchronization.

5.3.3 Grid-connected

Normal

During grid-connected mode the voltage components are assumed to be aligned with the d axis, to maintain the alignment the RSL stays connected ensuring the current components and the active and reactive power are decoupled. A reference is given for the active power and the reactive power is controlled to remain at zero.

The references of the outerloop are the active power reference on d loop with active power measurement on the feedback, and zero value reference on the q loop with reactive power measurement on the feedback.

The RSL is on in its grid frequency tracking mode during its steady state period, maximum frequency variation is reduced to improve performance in case of failures.

Unintentional islanding

If the system is operating in grid-connected mode and suddenly losses the grid, before it is noticed, it would try to control the power components unsuccessfully causing the voltage components to drift and get misaligned. To avoid this from happening the control of the q component is changed from reactive power to the q component of the voltage if this component has an absolute value higher than a threshold. While this action is active the d component is set to regulate the voltage as long as the q component error is present. This condition is called an unintentional islanding and is controlled like in the islanding case but without disconnecting from the grid and with the presence of a small alignment error.

If the grid is quickly recovered then the error will gradually reduce and again it will operate in grid-connected mode. If the condition remains then the Anti-Islanding Protection will detect it after the specified period of time and the inverter will work in islanded mode.

The RSL will have as input the voltage that the inverter alone is producing, since there is a small error in the q component of the voltage a small deviation from the nominal frequency will happen, by having a smaller maximum frequency variation during operation than during reconnection this deviation can be kept to a very small value, thus maintaining the system at nominal frequency during the fault.

The references of the outerloop are the voltage magnitude reference on d loop with d component of the voltage on the feedback, and zero value reference on the q loop with q component of the PCC voltage on the feedback.

The RSL is on with an output with a small offset.

Chapter 6

Stability of operation

This chapter analyses the results from the simulation of the microgrid with the structure and control described in the previous chapters. The behaviour of the current is discussed, and the stability of the system is studied.

6.1 Control Stability

With the adequate selection of PI parameters for each of the control loops, and considering the characteristics of the filter and the load the system was studied in the frequency domain to predict its stability through an analysis of the location of the roots of the system. Figure 6.1 presents the root locus plots for the inner control loop and the the power and voltage control loops considering the inner control in them. It can be observed by the location of the poles, that the proposed control remains stable.

6.2 Simulations

6.2.1 Start of Operation

When the system starts to islanded operation mode the local load is initially powered down. The inverter will start its operation in normal islanded mode and quickly, yet gradually, increase the current until the desired voltage is obtained at the output while ensuring its correct alignment with the d axis. The behaviour of the current can be observe in figure 6.2 where no overcurrents are observed.

To start working when the local load is already connected to the grid then the voltage reference given by the controller is matched to that of the grid. This is achieved activating the RSL and waiting for the synchronization signal, after which the system can be turned on in grid-connected mode. As observed in figure 6.3, there is an initial current present due to the capacitor from the LCL filter and the current gradually increases to provide the set-point power injection. Again

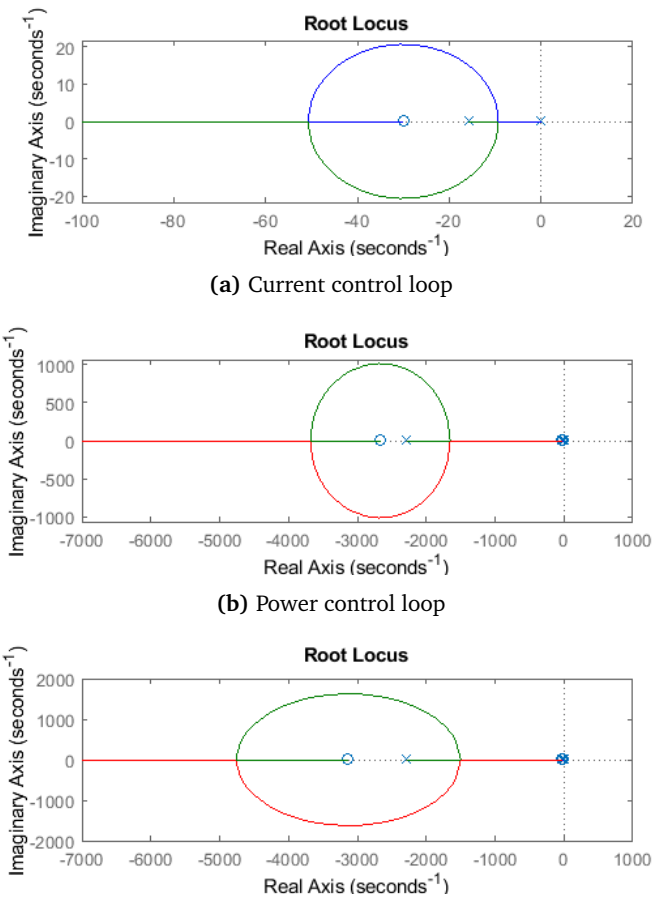

(a) Current control loop

(b) Power control loop

(c) Voltage control loop

Figure 6.1: Root Locus of the control loops used

no undesirable behaviours are observed and the start of operations is completely seamless.

6.2.2 Transition from islanded mode

If the system is operating in islanded mode and it needs to be connected to the grid, then the inverter will begin to quickly synchronize and match voltage, frequency and phase with little to no error. The system can seamlessly reconnect after this process and change its operation mode from islanded to grid-connected. The current smoothly changes to follow the new set-point without any signs that the reconnection ever happened as observed in figure 6.4c. The frequency of the microgrid varies within the specified limits, in this example between 48 Hz and 52 Hz to achieve the synchronization as observed in figure 6.4b

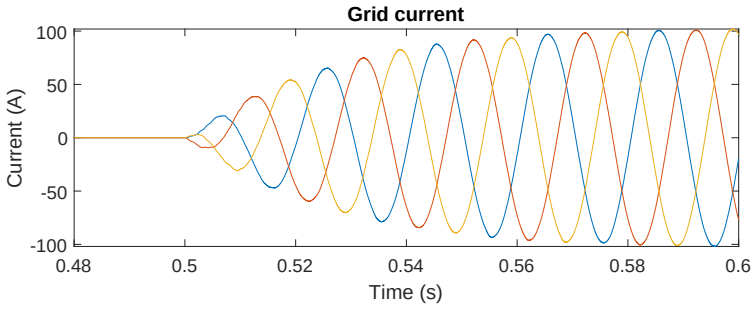

Figure 6.2: Current during start to islanded mode

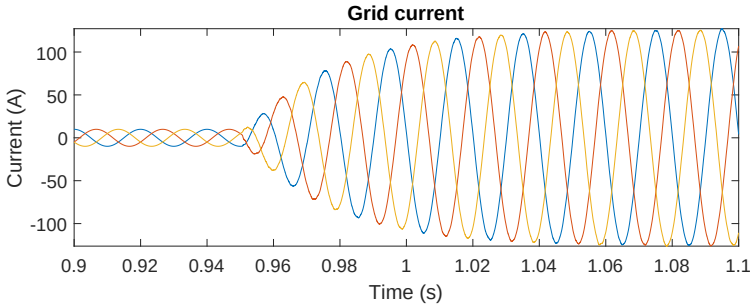

Figure 6.3: Current during start to grid-connected mode

6.2.3 Grid-loss During Grid-connected mode

If the grid fails during operation, the system will be effectively islanded without noticing it. At the moment of the fault the voltage will suddenly rise or drop and the current will rise or drop depending on how the local load compares to the set-points. The overvoltage can be observed in figure 6.5a. Since the system will be trying to control the power in an islanded system a small misalignment from the voltage will occur which will be reflected in the frequency, by using a small droop during grid-connected mode this error is greatly limited, see figure 6.5b, and when the grid is recovered at time 2.75 s no overcurrents are observed, see figure 6.6a. If the islanded condition is sustained, then the AIP [9] detects the fault and disconnects from the grid, going back to a constant frequency reference, see figure 6.5c.

6.2.4 Resynchronization with UDC model

The UDC resynchronization method proposed in [14] uses a virtual current just like the RSL block used in this paper, so it is a technique with many similarities to the one here presented. A simulink simulation with the UDC was ran to observe its performance during resynchronization. The results from this simulation are as expected similar in both the current and frequency behaviour to the ones obtained with the RSL. Figure 6.7 shows the frequency and current with this model.

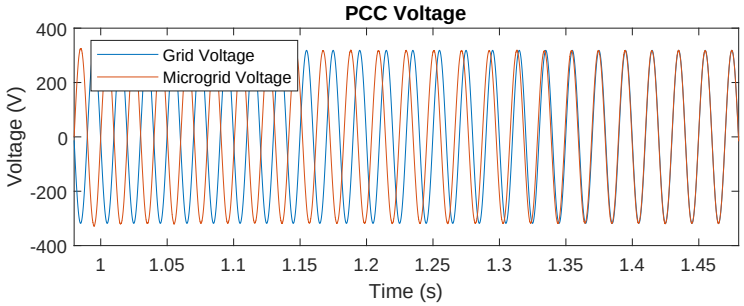

(a) Voltages

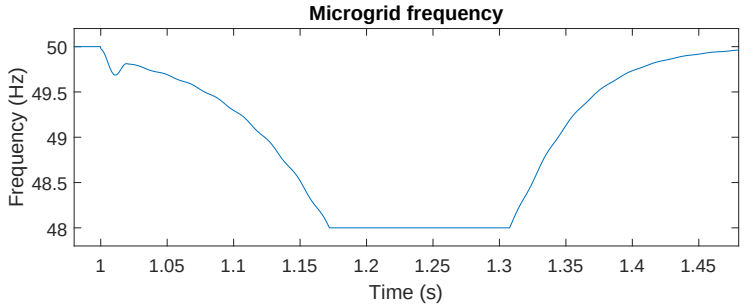

(b) Frequency

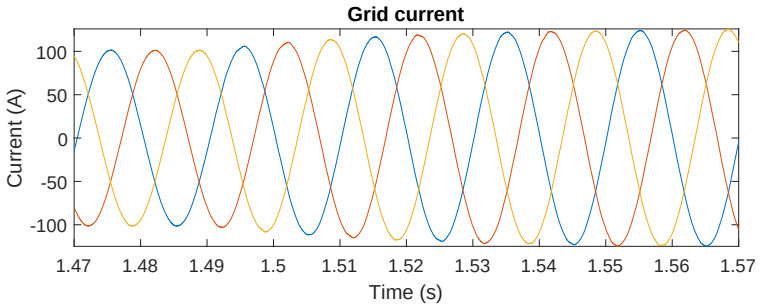

(c) Current during reconnection

Figure 6.4: Resynchronization during islanded mode

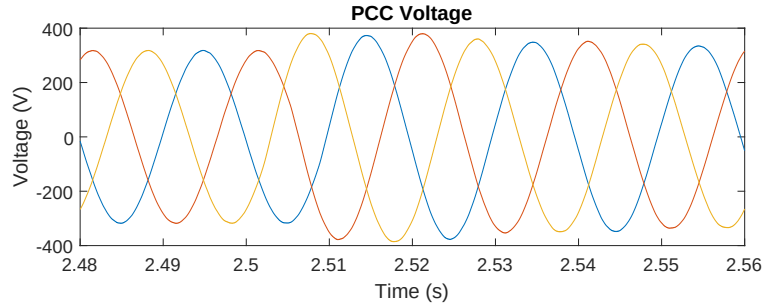

(a) Voltage at fault instant

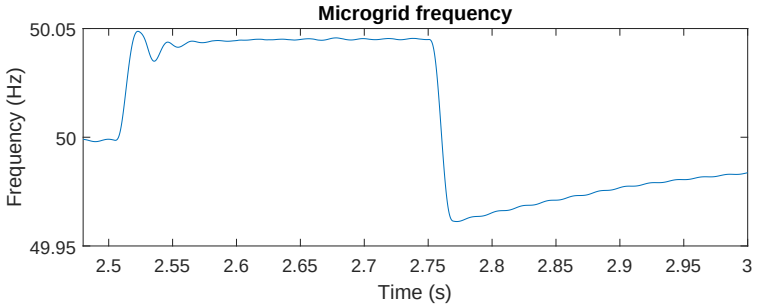

(b) Frequency during short grid-loss

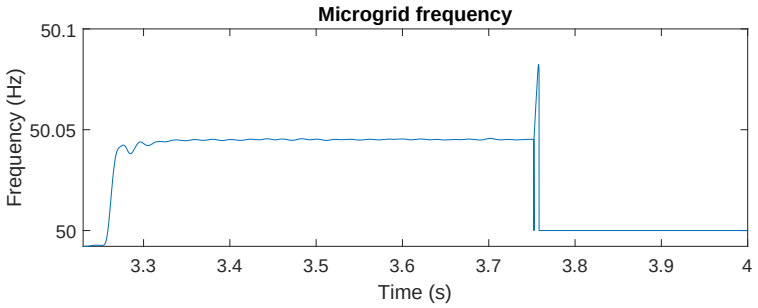

(c) Frequency during long grid-loss

Figure 6.5: Transient during grid-loss events

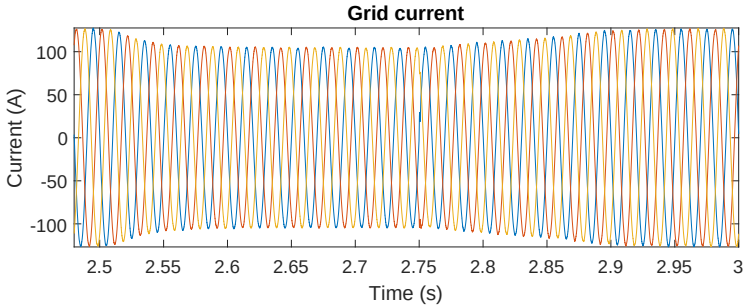

(a) Short grid-loss

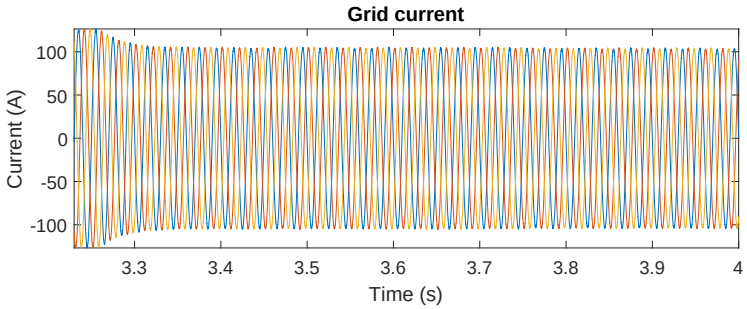

(b) Long grid-loss followed by islanded operation

Figure 6.6: Current behaviour during grid-loss

One of the advantages of the method proposed here against the UDC re-synchronization method is that there is no need for two synchronization blocks for the tasks of connection and reconnection, as the RSL does the work in both cases.

6.3 Steady State Operation

The system is able to correctly follow its references during the islanded or grid-connected modes, the BESS is able to correctly regulate the DC bus voltage dampening the variations from the PV system. The inverter operates as if fed by a constant source. While connected it correctly tracks the grid and remains aligned.

6.4 Reconnection

The reconnection is achieved quickly and seamlessly, by having a small maximum frequency deviation the waveforms do not change noticeably. While the system adjusts to the grid conditions the operation remains stable and correctly continues to feed the local load. Finally, when reconnected, the transition to following the power references instead of the voltage references is done smoothly and seamlessly, so there are no harmful overcurrents or sudden voltage drops.

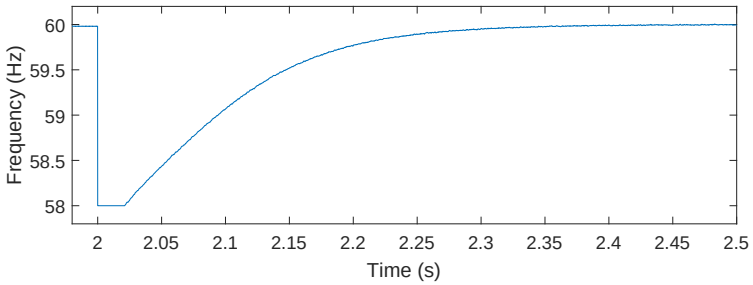

(a) Frequency during synchronization

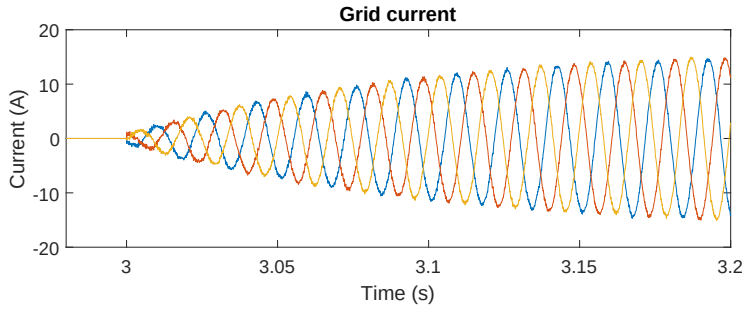

(b) Current during reconnection

Figure 6.7: Transient during change from islanded mode to Grid-connected with UDC controller

6.5 Errors

If the grid is lost during grid-connected operation, the system is able to operate within the specified limits until the islanding condition is detected and the system starts to operate in islanded mode. If the grid is lost at the critical moment when the microgrid is resynchronizing with the grid, it interrupts the process and returns to normal islanding operation.

Chapter 7

Conclusions

This chapter contains the conclusions drawn from the observed performance and the analysis of the results. It presents how the objectives of this work are achieved and presents some final remarks regarding the possible applications and limitations of the proposed scheme. It concludes with possible topics for further research based on the delimitations of this study.

7.1 Concluding Remarks

The desired objective of reconnecting a microgrid to the grid seamlessly was achieved with satisfactory results; small renewable power plants can benefit from being part of a microgrid when they are located near the shore. The two processes needed for it, i.e. the synchronization, and the reconnection, both happen without noticeable effect on the grid, other than a controlled frequency variation and a possible small step change in the voltage reference.

The synchronization period is relatively short limiting the frequency variation to 2 hertz above or below the nominal value. It is in the same order as the resynchronization time of the UDC with the virtual-current-based synchronization block. It could be said that the use of the RSL leads to the equivalent in the vector control of the virtual current resynchronization used in the droop control.

The hybrid AIP system used on the microgrid model is able to efficiently detect the islanding condition, but is limited to microgrids with local loads with a reactive component as it could miss the detection of the islanding condition if the active power setpoint were close to the local load demand.

The microgrid is able to remain stable when unintentionally islanded, with only a small misalignment of the voltage components, displaying a robust behaviour during faults and sudden recovery of the grid. It is also able to start working in any of the two modes in a seamless manner.

The way the control is implemented is light-weight, with minimal modifications from the classic vector control technique. The RSL block is simple and is not a cause for concern as the PLL usually is. The stateflow chart that controls the operation condition of the inverter performs simple calculations and does not greatly increase the overall complexity.

The control method proposed in this document could help small nearshore wind farms and tidal generation systems to integrate better into the network by allowing it to easily supply the energy required by local loads while simplifying its interface to the main grid.

7.2 Further research

Considering the limitations of this work and the results obtained from the different simulations presented in this thesis some topics of future work have been identified. Here the subjects are briefly presented.

The RSL block used in this study is slower than a PLL. Further work could be done in studying its behaviour in grids with constant frequency variations like those in islands where renewable energy sources are predominant. By allowing for larger frequency variations the RSL block works faster so an analysis of what the compromises that are made when modifying the speed of the RSL could be done.

The AIP system has a short delay to avoid false islanding conditions that would disconnect the microgrid even when no faults occurred. The main reason for this delay is that it is needed to comply with Low Voltage Ride-Through (LVRT) requirements. A more complete study of the proposed control during this kind of faults would be necessary to ensure that it is able to remain operational during the times specified in the grid codes.

A hardware in the Loop test of the microgrid model and control would help validate the proposal and improve the technological readiness of this controller.

Study of the interaction of several RSL-based microgrids in a network. The feasibility of this proposal was proven with a single inverter connected to the grid, but future work can be developed in how more microgrids would interact when connected to the grid or when forming a grid between themselves. Of special interest would be the ability of the group of microgrids to detect an islanding condition.

Bibliography

[1] *Data & Statistics*, en-GB. [Online]. Available: https://www.iea.org/data-and-statistics/data-browser (visited on 26/06/2021).

[2] *Microgrid Defined: Three Key Features that Make a Microgrid a Microgrid*, en-US, Section: About Microgrids, Jun. 2020. [Online]. Available: https://microgridknowledge.com/microgrid-defined/ (visited on 12/11/2020).

[3] H. Xu, X. Zhang, F. Liu, D. Zhu, R. Shi, H. Ni and W. Cao, 'Synchronization strategy of microgrid from islanded to grid-connected mode seamless transfer,' in *2013 IEEE International Conference of IEEE Region 10 (TENCON 2013)*, ISSN: 2159-3450, Oct. 2013, pp. 1–4. DOI: 10.1109/TENCON.2013.6718475.

[4] *Implement PV array modules - Simulink - MathWorks Nordic*. [Online]. Available: https://se.mathworks.com/help/physmod/sps/powersys/ref/pvarray.html (visited on 24/05/2021).

[5] M. A. Elgendy, B. Zahawi and D. J. Atkinson, 'Assessment of the Incremental Conductance Maximum Power Point Tracking Algorithm,' *IEEE Transactions on Sustainable Energy*, vol. 4, no. 1, pp. 108–117, Jan. 2013, Conference Name: IEEE Transactions on Sustainable Energy, ISSN: 1949-3037. DOI: 10.1109/TSTE.2012.2202698.

[6] V. Mummadi, 'Improved maximum power point tracking algorithm for photovoltaic sources,' in *2008 IEEE International Conference on Sustainable Energy Technologies*, ISSN: 2165-4395, Nov. 2008, pp. 301–305. DOI: 10.1109/ICSET.2008.4747021.

[7] M. Dursun and M. K. DÖŞOĞLU, 'LCL Filter Design for Grid Connected Three-Phase Inverter,' in *2018 2nd International Symposium on Multidisciplinary Studies and Innovative Technologies (ISMSIT)*, Oct. 2018, pp. 1–4. DOI: 10.1109/ISMSIT.2018.8567054.

[8] *Vector control for dummies*, en-US. [Online]. Available: https://www.switchcraft.org/learning/2016/12/16/vector-control-for-dummies (visited on 22/06/2021).

[9] M. Amin, Q.-C. Zhong and Z. Lyu, 'An Anti-Islanding Protection for VSM Inverters in Distributed Generation,' *IEEE Open Journal of Power Electronics*, vol. 1, pp. 372–382, 2020, Conference Name: IEEE Open Journal of Power Electronics, ISSN: 2644-1314. DOI: 10.1109/OJPEL.2020.3021288.

[10] Y. Zhang, R. A. Dougal and H. Zheng, 'Tieline Reconnection of Microgrids Using Controllable Variable Reactors,' *IEEE Transactions on Industry Applications*, vol. 50, no. 4, pp. 2798–2806, Jul. 2014, Conference Name: IEEE Transactions on Industry Applications, ISSN: 1939-9367. DOI: 10.1109/TIA.2013.2294998.

[11] T. Uten, C. Charoenlarpnopparut and P. Suksompong, 'Synchronization Control for Microgrid Seamless Reconnection,' in *2019 14th International Joint Symposium on Artificial Intelligence and Natural Language Processing (iSAI-NLP)*, Oct. 2019, pp. 1–6. DOI: 10.1109/iSAI-NLP48611.2019.9045428.

[12] C. Cho, J. Jeon, J. Kim, S. Kwon, K. Park and S. Kim, 'Active Synchronizing Control of a Microgrid,' *IEEE Transactions on Power Electronics*, vol. 26, no. 12, pp. 3707–3719, Dec. 2011, Conference Name: IEEE Transactions on Power Electronics, ISSN: 1941-0107. DOI: 10.1109/TPEL.2011.2162532.

[13] D. Shi, X. Chen, Z. Wang, X. Zhang, Z. Yu, X. Wang and D. Bian, 'A Distributed Cooperative Control Framework for Synchronized Reconnection of a Multi-Bus Microgrid,' *IEEE Transactions on Smart Grid*, vol. 9, no. 6, pp. 6646–6655, Nov. 2018, Conference Name: IEEE Transactions on Smart Grid, ISSN: 1949-3061. DOI: 10.1109/TSG.2017.2717806.

[14] M. Amin and Q.-C. Zhong, 'Re-synchronization of Universal Droop Control Distributed Generation Inverter to the Grid,' in *2019 IEEE Energy Conversion Congress and Exposition (ECCE)*, ISSN: 2329-3748, Sep. 2019, pp. 4435–4440. DOI: 10.1109/ECCE.2019.8912518.

[15] Q.-C. Zhong, 'Robust Droop Controller for Accurate Proportional Load Sharing Among Inverters Operated in Parallel,' *IEEE Transactions on Industrial Electronics*, vol. 60, no. 4, pp. 1281–1290, Apr. 2013, Conference Name: IEEE Transactions on Industrial Electronics, ISSN: 1557-9948. DOI: 10.1109/TIE.2011.2146221.

[16] Q.-C. Zhong and Y. Zeng, 'Universal Droop Control of Inverters With Different Types of Output Impedance,' *IEEE Access*, vol. 4, pp. 702–712, 2016, Conference Name: IEEE Access, ISSN: 2169-3536. DOI: 10.1109/ACCESS.2016.2526616.

[17] Q.-C. Zhong, W.-L. Ming and Y. Zeng, 'Self-Synchronized Universal Droop Controller,' *IEEE Access*, vol. 4, pp. 7145–7153, 2016, Conference Name: IEEE Access, ISSN: 2169-3536. DOI: 10.1109/ACCESS.2016.2616115.

[18] M. Amin, 'A Robust-Synchronization-Loop for Grid-Connected Distributed Generation Converters,' in *IECON 2020 The 46th Annual Conference of the IEEE Industrial Electronics Society*, ISSN: 2577-1647, Oct. 2020, pp. 3648–3653. DOI: 10.1109/IECON43393.2020.9255190.

Appendix A

Parameters of the microgrid

A.1 Photovoltaic System

Table A.1: Values for PV model

Parameter	Value	Unit
# of modules	470	1
modules per string	10	1
# of strings	47	1
Open circuit voltage	36.3	V
Short circuit current	7.84	A
Voltage at maximum power point	29	V
Current at maximum power point	7.35	A
Nominal irradiance	1	$\frac{kW}{m^2}$
Temperature	25	^oC
Power	100	kW
Boost switching frequency	5	kHz
Boost inductor	1.7	mH
Boost capacitor	2.1	mF

A.2 Battery Energy Storage System

Table A.2: Values for BESS model

Parameter	Value	Unit
Power	100	kW
Battery voltage	300	V
Voltage reference	800	V
Converter switching frequency	5	kHz
Converter inductor	1.7	mH
Converter capacitor	2.1	mF

A.3 LCL Filter

Table A.3: Values for LCL filter model

Parameter	Value	Unit
Power	100	kW
Filter frequency	10	kHz
DC voltage	800	V
AC voltage	400	V
Modulation index	0.8165	1
Resonant frequency	4.1	kHz
Inverter-side inductor	1.3	mH
Inverter-side resistor	20	$m\Omega$
Grid-side inductor	15.3	μH
Grid-side resistor	0.24	$m\Omega$
Capacitor	100	μF
Filter resistor	130	$m\Omega$

Appendix B

Matlab/Simulink Models

B.1 Photovoltaic System

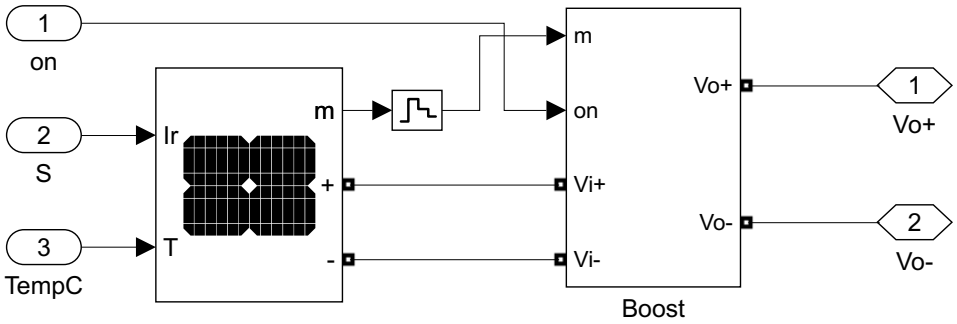

Figure B.1: PV model

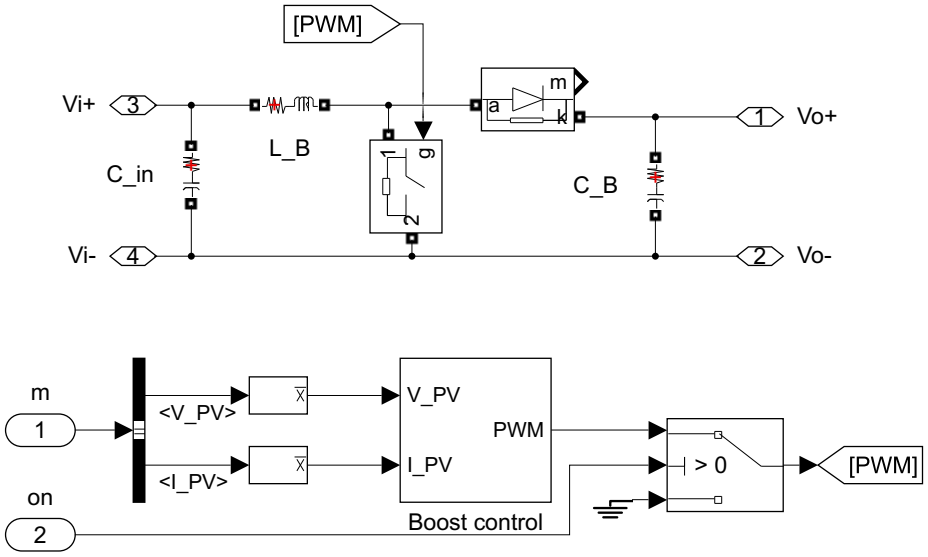

Figure B.2: MPPT-Boost converter model

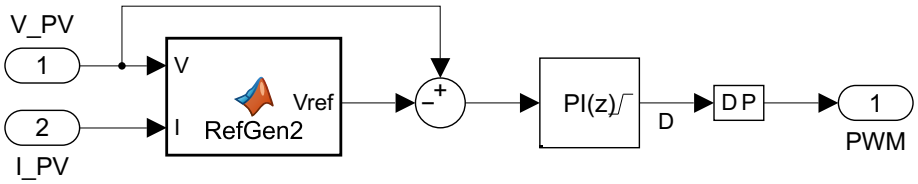

Figure B.3: MPPT-Boost control model

B.2 Battery Energy Storage System

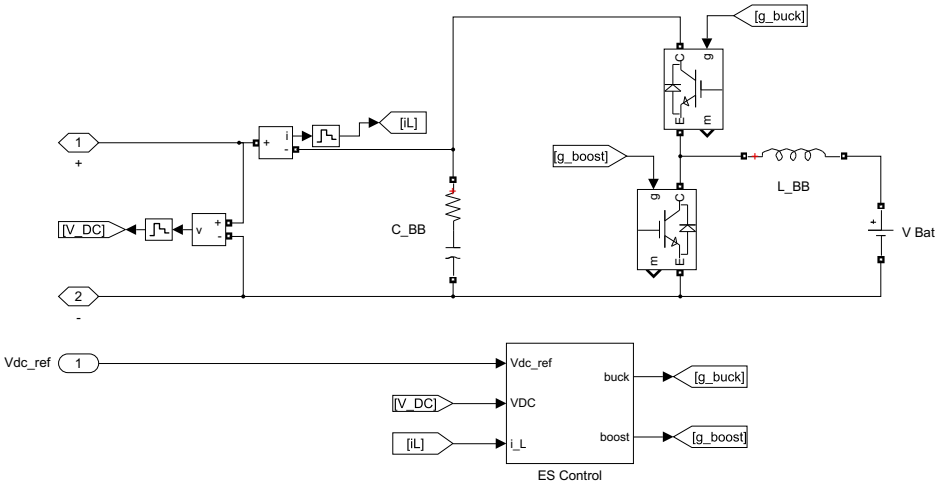

Figure B.4: BESS model

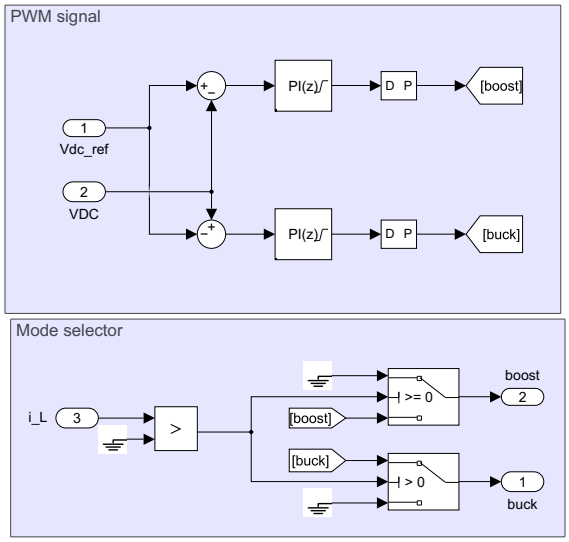

Figure B.5: BESS control model

B.3 Inverter

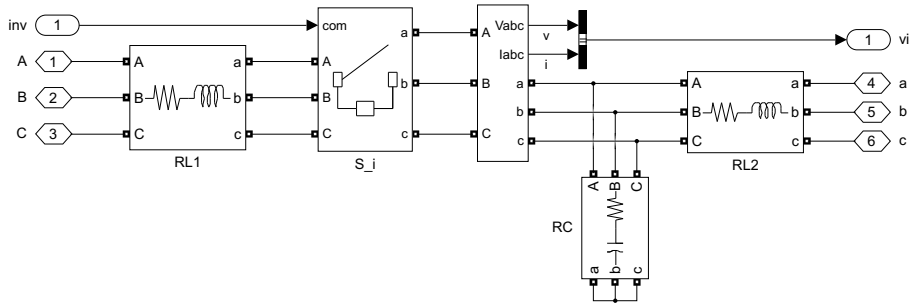

Figure B.6: LCL model

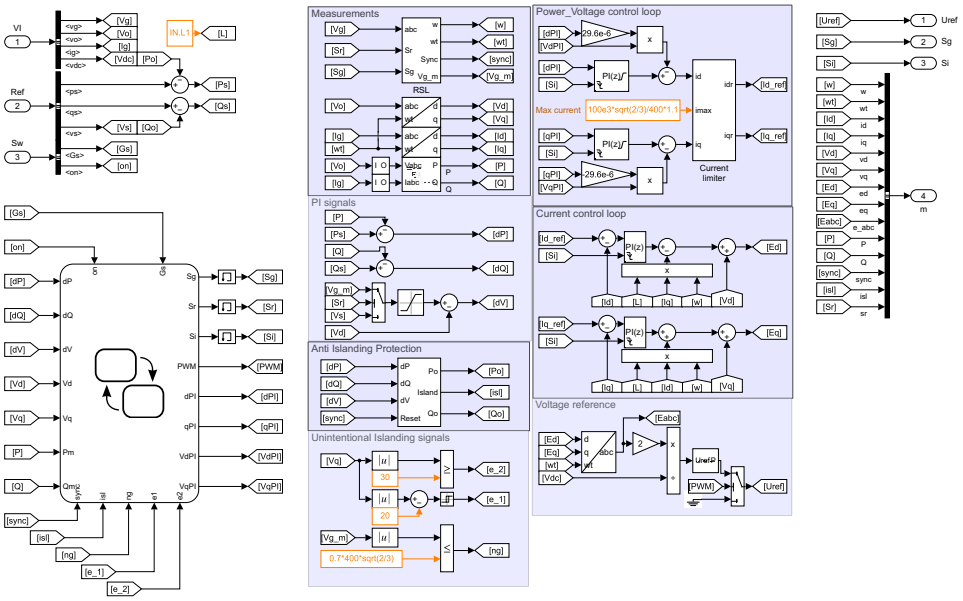

Figure B.7: Inverter control implementation

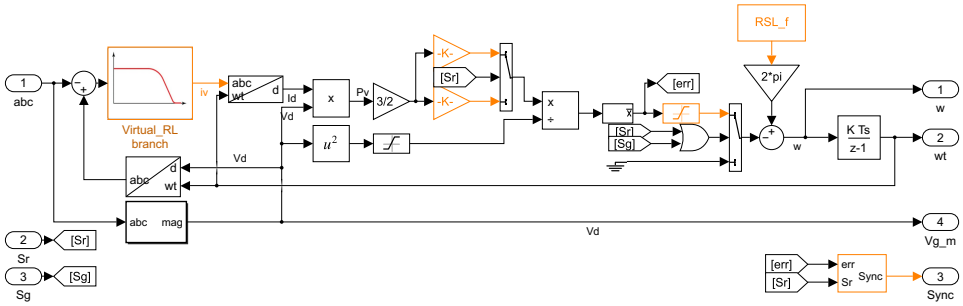

Figure B.8: RSL model

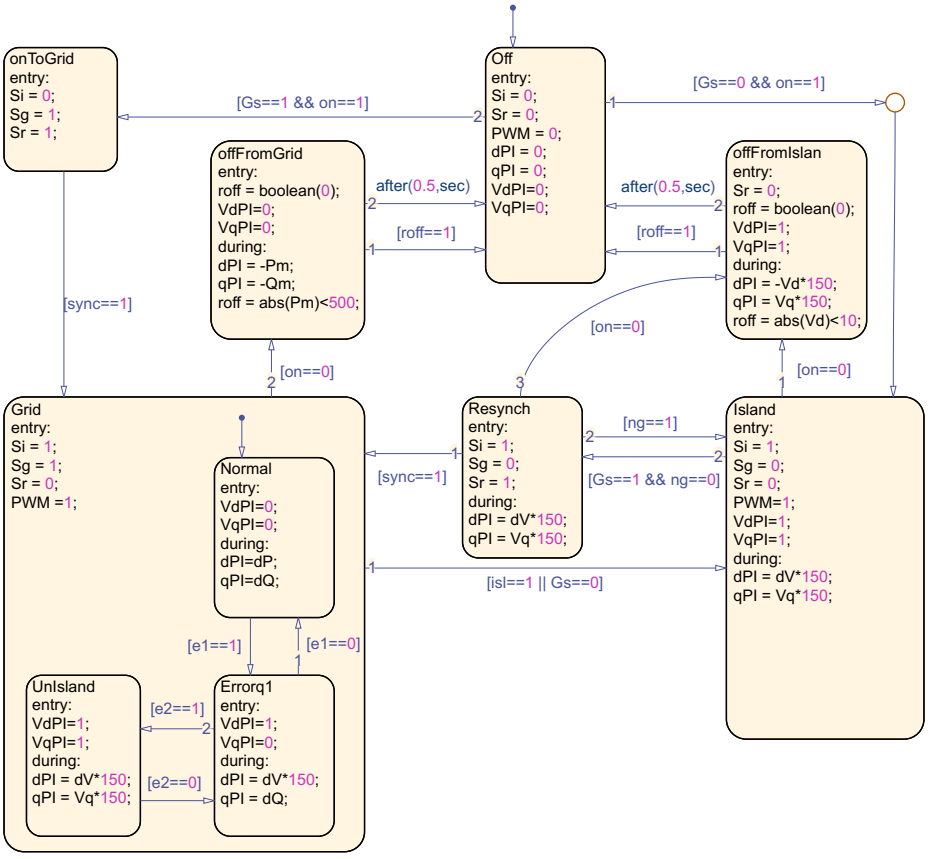

Figure B.9: Operation stateflow model

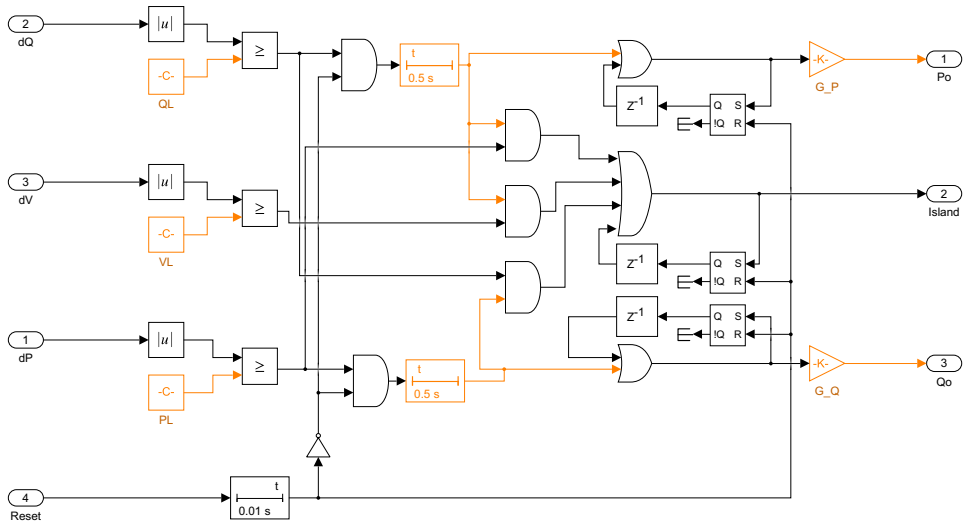

Figure B.10: AIP model

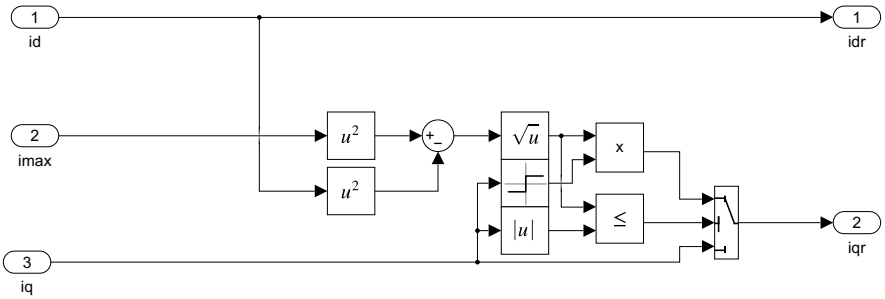

Figure B.11: Current limiter model

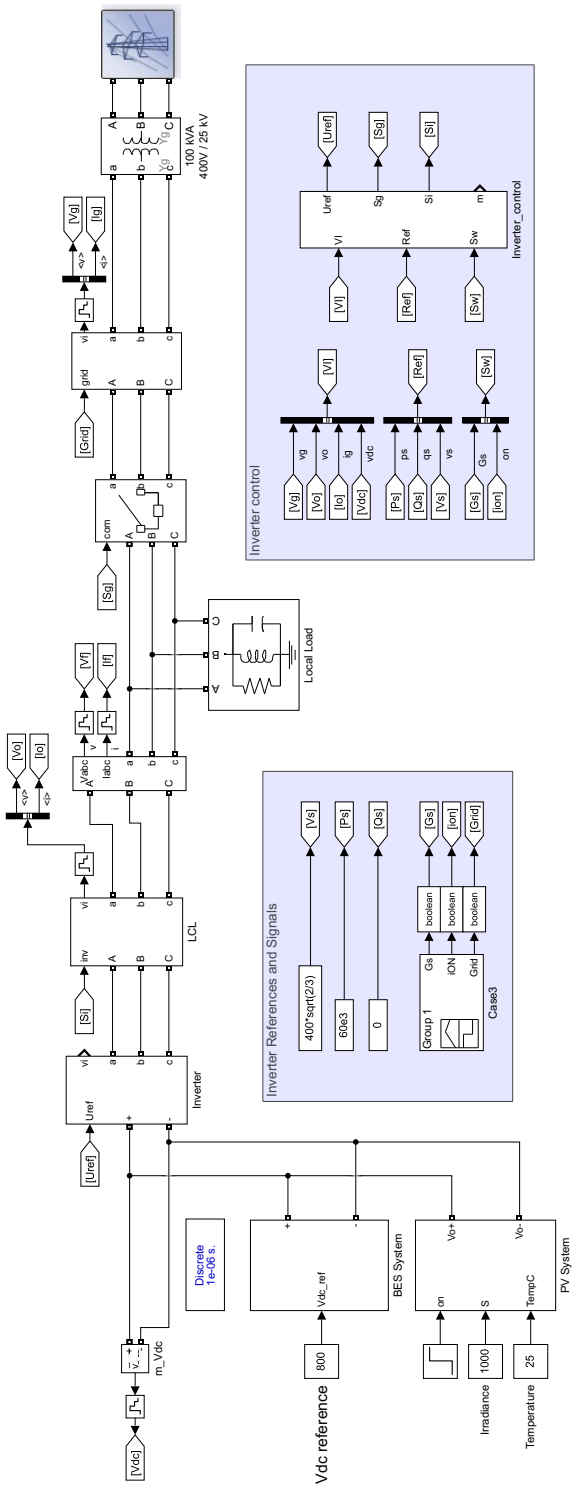

Figure B.12: Microgrid model

Appendix C

Scientific paper

Paper I

Seamless Microgrid Reconnection with RSL block

Rafael Marentes-Ortiz, *Student, NTNU*

***Abstract*—In this paper, the current proposals to seamlessly reconnect a microgrid to the grid are presented, along with their characteristics and requirements. The advantages and drawbacks of each are discussed and their performance is compared. A microgrid model with a photovoltaic system and a battery energy storage system connected to a DC bus is used. An inverter with a Robust Synchronization Loop (RSL) is then proposed to operate and synchronize the microgrid to the grid. The modifications needed and the control for each operation mode are discussed along with an analysis of the stability of the system. The effectiveness of this implementation is then proved with simulations in Matlab/Simulink.**

***Index Terms*—microgrid, synchronization, SSSC, simulink, powersim.**

I. Introduction

THERE have been several proposals to address the obstacles encountered when microgrids change operation modes. In this document some of this proposals are analysed and discussed, and some new ideas are developed and compared to the existing solutions to study their feasibility.

A. Microgrids

A microgrid is an energy system made up of distributed generation, storage systems and local loads in a specific geographic location. Microgrids are self-sufficient systems, capable of providing for their own energy needs; nonetheless, they are usually connected to the main grid. There are three characteristics that define a microgrid:

1) Local: The energy sources and sinks are in close range, there is usually no need for a large transmission system. The main advantage here being the low power losses caused by the transmission and distribution of the energy.

2) Independent: The microgrid has islanded capability and can run even in the absence of the main grid, bringing resilience to the network in case of faults. This independence do not mean that the microgrid will not attempt to remain connected to the grid. It is beneficial for both systems to operate connected, strengthening both grids and giving the possibility of power transfer, if necessary.

3) Intelligent: The production inside a microgrid is determined by algorithms that optimize price, reliability, pollution, etc. The microgrid controller sets the overall behaviour and decides on purchasing and selling energy should it result convenient to the performance of the microgrid. The ability of the microgrid to work independently represents, as it was mentioned, a huge advantage, but also a challenge. When the microgrid operates islanded, despite its voltage and frequency controls, the electric parameters drift away from the main grid ones, resulting in unwanted transitory currents that destabilize the system if reconnected. Therefore, a process must be carried out to effectively achieve the reconnection to the grid. To reconnect the two systems, it is necessary to match the electric parameters of the grid at the point of common coupling (PCC), these parameters are: frequency, phase and voltage magnitude. The process by which this is achieved is known as synchronization. To supply the electric demand without interruptions, it is of the utmost importance for the microgrid to be able to operate in both, grid-connected and islanded, modes with smooth transitions between them [1], [2].

R. Marentes studies at the Department of Electrical Engineering, NTNU, Trondheim, 7491 Norway e-mail: rafaelm@stud.ntnu.no

Manuscript delivered June 1, 2021.

B. Synchronizing methods

Several methods have been proposed to address the challenge of reconnecting a microgrid. These methods are diverse and mostly differ in which elements are assumed to be available. If a large-area communication network is present, the distributed generation can be controlled to drive the electric conditions to the desired ones [3]. However, this can be a very slow process, especially if the system has generators with large inertia. C. Cho [4] proposed a control scheme where offset signals are sent to all controllable DGs to distribute the burden of synchronizing the microgrid. The technique was tested with some renewable sources, two Diesel Engines as DGs and a BESS. The generators would be commanded to modify their power injection to adjust the frequency and phase while the BESS would compensate by absorbing the extra power injected in the system. Their result was that in less than 6 seconds the system was able to successfully synchronize but not without some observable power oscillations. It was noted that the communication delay could have large impacts, as too long delays led to system instability. Other methods that are insensitive to communication latency have been proposed by [5] sending to all controllable generators the same reference to eliminate the phase difference at the PCC in about 5 seconds. When a communication network is not present or is undesirable for economic reasons, methods that do not rely on it are developed. One such approach is [6] where an additional generation system, referred to as a Dispatch Unit (DU), is used to drive the microgrid towards synchronization. This DU is connected at the PCC and is controlled to generate the necessary power to adjust the electric parameters with those of the grid. With a size of 2.5% of the aggregate capacity of the microgrid it is able to achieve synchronization in under 5 seconds in a seamless manner. The main disadvantage of this method is the need for an extra machine to operate only when reconnecting is needed, and whose cost increases as the size of the microgrid increases. Another method that has been proposed is the use of variable reactor devices. These devices

TABLE I
IEEE 1547 STANDARD FOR GRID RECONNECTIONS

Average Power $[MW]$	Frequency difference [Hz]	Voltage difference [pu]	Phase difference [°]
0 – 500	0.3	0.1	20
501 – 1500	0.2	0.05	15
1501 – 10000	0.1	0.03	10

are usually utilized to control power flow, and to improve the power quality by, for example, dampening oscillations. They consist of a fixed reactance switched by mechanical or electronic means. Examples of these are, the thyristor-controlled reactor (TCR), the rotational magnetic core variable reactor (RMC-VR) and the virtual air-gap variable reactor (VAG-VR). The TCR is usually used as a flexible AC transmission system (FACTS) operated by varying thyristor firing angles, resulting in high harmonic distortion. The RMC-VR and VAG-VR lack this disadvantage and were considered more appropriate for microgrids in the proposal made by Zhang et al. [7]. Of these two, the virtual air-gap device has a wider range and a faster response, so it is therefore a better option for synchronization purposes. The value of the variable reactance is controlled to minimize the initial power flow following the reconnection. With this method a reduction of 90% of the peak current during reconnection was achieved, with a significant reduction in voltage and frequency oscillations. This method nonetheless does not provide a truly seamless transition. A technique proposed for inverter-based distributed generators controlled with the Universal Droop Controller (UDC) is to add to the current measurement a value which is proportional to the current that would flow between the grid and the microgrid through a virtual branch, since the microgid is only providing power to the local load, the system will adjust the voltage and frequency to minimize this virtual current, therefore eliminating the error at the PCC, allowing for a smooth reconnection. Since this procedure is proposed for an inverter, it is able to achieve the synchronization criteria very quickly, in less than a second. The advantages of this technique are that it does not require a communication network and that by using the UDC it also does not require a PLL block which results in a very stable operation. The main limitation of this method is that the droop control leads to a small steady-state error.

Even with the best controllers, the electric conditions will never be exactly the same on both grids, so tolerances are considered and specified in the IEEE 1547 standard summarized in table I.

C. Article Structure

This article mainly deals with a novel reconnection technique for inverter-based microgrids which utilizes a modified PLL-like block to seamlessly reconnect to the grid. An introduction to microgrids is first presented in this section, followed by a short overview of the current synchronization methods, their results and limitations. This is followed by an explanation of the components of the microgrid, and the structure and operation of the RSL block which provides the frequency and voltage references that enable the synchronization. A detailed description is then given of the operation modes of the microgrid and the control scheme proposed for each mode accompanied of simulation results that verify the stable operation of the microgrid in all modes and the effectively seamless transition between operation modes. The control models are presented to prove its stability from a mathematical point of view and the results from the simulations are further explained. Finally, conclusions are drawn based on what was observed.

II. MICROGRID MODEL

The microgrid has three main elements: a photovoltaic system that provides the power, a battery energy storage system to regulate the DC bus voltage, and an inverter to inject the energy to a local load and the grid. The photovoltaic system consists of a series of panels whose output is controlled by a boost converter that regulates the voltage according to a maximum power point tracker (MPPT) algorithm. This system outputs variable power depending on the temperature and solar irradiance and injects it into the DC bus. The BESS regulates the bus voltage to a reference by absorbing energy through a buck converter or injecting it through a boost converter, both implemented with a half bridge topology sharing the same inductor. The inverter is controlled by sinusoidal pulse width modulation, obtained from a current controller that operates on the current components in the dq frame. The effect of each component is decoupled to control the frequency, voltage, and active and reactive powers.

A. Photovoltaic

A photovoltaic system as a distributed generation source is proposed. The number of modules is initially chosen to provide 100 [kW] with a 1 [kW/m²] irradiance. A boost converter is connected at the output to control the PV voltage near its optimal value of 290 [V]. The boost converter components are determined by the design procedure considering the output power of the PV array, the PV voltage range, current and voltage ripples, and an arbitrarily set frequency of 5 kHz. The output of the boost converter is connected to an 800 V DC bus.

1) Boost Converter: The selected parameters to test the component are:

$$
\begin{aligned}
V_i &= (250 \Leftrightarrow 350)[V] \\
V_o &= 800[V] \\
P &= 100[kW] \\
fs &= 5[kHz] \\
\Delta I &= 5\% I_{max} = 5\% \frac{P}{V_{i\,min}} \\
\Delta V &= 1\% V_o
\end{aligned}
$$

The design equations for the boost converter are:

$$L = \frac{V_{i_{min}} \cdot (V_o - V_{i_{min}})}{f_s \cdot \Delta I \cdot V_o} \qquad = 1.72[mH]$$
$$C = \frac{I_o \cdot (V_o - V_{i_{min}})}{f_s \cdot \Delta V \cdot V_o} \qquad = 2.1[mF]$$

2) Control: A PI control was used to define the duty cycle, increasing it if the terminal voltage of the PV array was higher than desired, or decreasing it if the voltage was lower. The voltage reference is generated with an MPPT algorithm of the incremental conductance type.

B. BESS

This device is simulated with a constant voltage source connected to the DC grid through a buck-boost converter, the control decides to inject or absorb energy into the bus depending on the voltage level therefore maintaining it constant regardless of the power injected by the PV system and the inverter. The design equation for the converter is the same as before, so the inductor can be calculated with the same equation. The voltage of the battery is set as 300 V, and the frequency of the PWM is set to 5 kHz.

$$I_o = \frac{P}{V_o} = \frac{100kW}{300V} \qquad = 333.3A$$
$$\Delta I = 5\% I_o \qquad = 16.7A$$

The inductor needed for this converter is the following one.

$$L = \frac{V_o \cdot (V_i - V_o)}{f_s \cdot \Delta I \cdot V_i} = \frac{300 \cdot (800 - 300)}{5000 \cdot 16.7 \cdot 800} \qquad = 2.25mH \quad (1)$$

C. Inverter

A standard universal bridge was selected for the inverter. The gate signals were determined with SPWM at a frequency of 10 [kHz]. The references were set by controlling the dq components of the current using the decoupling method. To generate these reference signals a PLL is needed to estimate the angle of the grid voltage.

1) RSL: The PLL-like block used is the Robust Synchronization Loop proposed in [8], which outputs a frequency reference and angle aligned those of the input signal, while displaying a stable and robust operation.

2) Control: Two PI control loops are defined, one for each component, at the output of the PI the product of the opposite current, frequency and inductance is added (or subtracted) as well as the corresponding grid voltage component in a feed-forward loop. The output is then scaled and transformed back to the abc frame to be used in the SPWM. The outer control loops depend on the operation mode of the microgrid.

3) LCL filter: To eliminate the high frequency harmonics from the PWM the inverter is connected to the grid through an LCL filter which is tuned to fullfill the parameters here specified:

$$P = 100kVA \qquad V_{DC} = 800V$$
$$V_{AC} = 400V \qquad f_s = 10kHz$$
$$k_a = 0.2 \qquad \Delta I = 10\% I_{max}$$

$$Z_b = \frac{V_{AC}^2}{P} \qquad = 1.6\Omega$$
$$C_b = \frac{1}{\omega_g Z_b} \qquad = 1.989mF$$
$$I_{max} = \sqrt{\frac{2}{3}} \frac{P}{V_{AC}} \qquad = 204A$$
$$\Delta I = 0.1 I_{max} \qquad = 20.4A$$

The design equations from [9] are:

$$C_f = 5\% C_b \qquad = 99.5\mu F$$
$$L_1 = \frac{V_{DC}}{6 f_s \Delta I_L} \qquad = 653\mu H$$
$$L_2 = \frac{\sqrt{\frac{1}{k_a^2}} + 1}{C_f \omega_s^2} \qquad = 15.27\mu H$$
$$R_f = \frac{1}{3} \sqrt{\frac{L_1 L_2}{C_f (L_1 + L_2)}} \qquad = 129m\Omega$$
$$M = \frac{2V_{AC}}{V_{DC}} \sqrt{\frac{2}{3}} \qquad = 0.817$$

All components calculated are per phase.

III. RSL BLOCK

A. Overview

The RSL block was proposed in [8] as a robust implementation of a PLL alternative. Its principle of operation is simulating the current in a virtual RL branch between the point where the voltage is measured and an estimated voltage. The active power is calculated with the estimated voltage and the calculated current assuming decoupled components, and the value of the calculated power is used to modify the measured frequency to minimize the power thus bringing the measured voltage and the estimated voltage to be the same. The output of the block are the frequency and angle used for the estimation.

B. Modifications and Signals

To use the block in the microgrid control some modifications were needed to operate it during islanded mode. The power measurement was disconnected so that the block would output a constant frequency reference. The frequency variation was limited to maintain the output within specification but the internal value was allowed to be large so that its operation could be fast and with smaller errors. The connection was controlled with a resynchronization signal which also enabled an output signal that turns on when the frequency variation is close to zero (around the specified frequency).

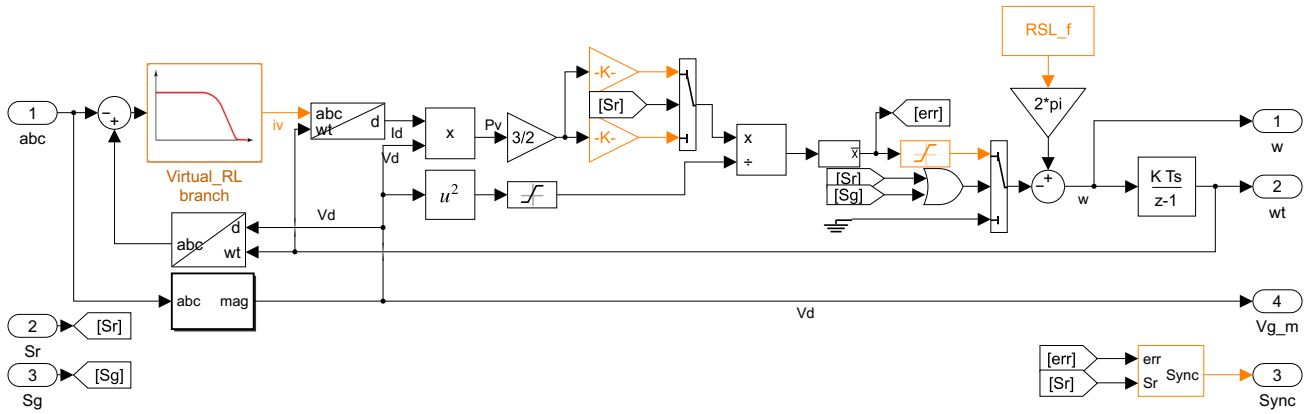

Fig. 1. RSL implementation in Simulink

C. Parameters and operation

The block receives as parameters: the nominal frequency, the resistance and inductance of the virtual branch and gain factor K, the maximum frequency variation, the maximum frequency variation allowed at the output, and the frequency threshold at which the synchronization signal would activate. With this parameters the model is configured and the droop constants calculated. a large droop constant is used during reconnection to quickly modify the state of the system, while a small droop constant is used during grid-connected mode to improve stability. In figure 1 the configurable blocks are highlighted in orange.

D. Limitations

The RSL block is able to correctly measure and track the input frequency, but has a steady state error in the phase at any frequency other than the nominal. This is because the output frequency is the result of a specified frequency and a variation proportional to the measured virtual power which exists only when there is a phase difference. Having a large maximum frequency variation reduces the phase error.

IV. Control

The control of the inverter that interfaces the microgrid with the AC system depends on the operation mode, as it is not possible to regulate the power when the system is islanded as this is determined by the load, and similarly in the grid-connected mode the frequency is determined by the grid. The inner-loop of the control remains unchanged for all operations but the outer-loop and the error signals will vary depending on different conditions.

A. Off

1) Normal: The PWM output is kept low and the PI compensators are turned off. The switch connecting the inverter to the system is opened and the switch connecting the local load to the grid can be either opened or closed.

2) Start to islanded: The microgrid quickly starts in islanded mode and follows the references without problems or undesirable behaviour. It can synchronize to the grid at any time by enabling the resynchronization signal.

a) Outerloop: Voltage control of V_d and V_q components.

b) References: V_d controlled to the set-point value V_s, and V_q controlled to zero.

c) RSL: Off. Provides constant frequency reference.

3) Start to grid-connected: Before starting the inverter when the grid is already connected to the local load it is necessary to set the internal references for the inverter voltage to the same ones at the PCC in order for the current to be zero when the system gets connected. Thanks to the structure of the current controller in the dq frame this voltage is already added to the reference and since it is off, the output of the PI is zero and there is no current, so the only thing needed to start the system is to align the d and q components of the voltage measured at the PCC. Simply turning the RSL block on achieves this. When the RSL is done synchronizing then the inverter output can be turned on and the inverter breaker closed.

a) RSL: On. With large frequency variation droop constant. Provides the necessary frequency variation to align the internal voltage reference for the initial connection.

B. Islanded

1) Normal: During the islanded operation, the voltage is determined not by the grid but by the currents injected in the equivalent impedance of the right half of the LCL filter and the local load. So for the nominal values of voltage and frequency, P and Q are fixed.

a) Outerloop: Voltage control of V_d and V_q components.

b) References: V_d controlled to the set-point value V_s, and V_q controlled to zero.

c) RSL: Off. Provides constant frequency reference.

2) Resynching: If the Grid-mode signal is active while operating in the islanded mode and the grid is present, then the synchronization process starts. The grid is detected by the presence of a voltage measurement above a specified threshold.

a) Outerloop: Voltage control of V_d and V_q components.

b) References: V_{dPCC} controlled to the grid measurement V_g, and V_{qPCC} controlled to zero.

c) RSL: On. With large frequency variation droop constant. Provides the necessary frequency variation to drive the system to the same phase as the grid.

C. Grid-connected

1) Normal: During grid-connected mode the voltage is set by the grid and thanks to the previous resynchronization process it is assumed to be aligned with the d axis. In this mode the control is over the injected powers. The RSL remains connected to correctly track frequency variations and maintain synchronization.

a) Outerloop: Power control of P and Q components.

b) References: P controlled to the power set-point P_s, and Q controlled to zero.

c) RSL: On. With small frequency variation droop constant. Tracks the frequency of the grid.

2) Unintentional islanding: If the system is operating in grid-connected mode and suddenly losses the grid, before it is noticed, it would try to control the power components unsuccessfully causing the voltage components to drift and get misaligned. To avoid this from happening the control of the d component is changed from active power to voltage once the q component exceeds a threshold and the q component is changed from reactive power to the q component of the voltage if this component exceeds a higher threshold. By doing it this way, the d component remains stable while the q component oscillates slightly around the defined threshold. If this condition is maintained for a certain period of time then the system considers it an unintentional islanding and sets its control to be as that of the islanding case without disconnecting from the grid. If it were not an islanding situation, or if the grid were quickly recovered then the error will go beyond the threshold and when this is detected it will operate in grid-connected mode again. If it is indeed an unintentional islanding case then the Anti-Islanding Protection will detect it after the specified period of time and the inverter will work in islanded mode and disconnect from the grid. The RSL will have as input the voltage that the inverter alone is producing, since there is a small error in the q component of the voltage a small deviation from the nominal frequency will happen, by having a smaller maximum frequency variation during operation than during reconnection this deviation can be kept to a very small value, thus maintaining the system at nominal frequency during the fault.

a) Outerloop: Dependent on the magnitude of the error. Voltage control during steady-state

b) References: Dependent on the magnitude of the error. V_d controlled to the set-point value V_s, and V_q controlled to zero in the steady-state.

c) RSL: On. With small frequency variation droop constant. Slight deviation from nominal frequency until unintentional islanding is detected.

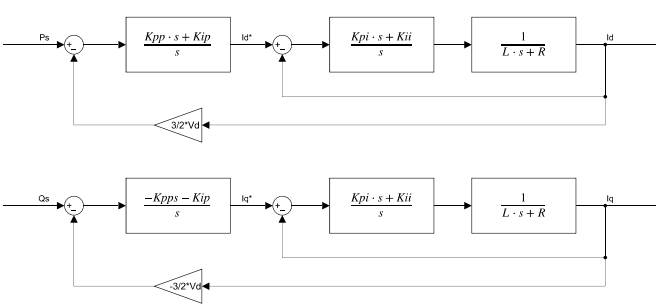

Fig. 2. Model of system and power control in the dq frame

V. Stability

A. Inner loop PI

By including the adequate signals after the current control PI the effects of the grid voltage and current is decoupled and the system can be seen as a PI block with an RL impedance, as seen also in the inner loop of figure 2. With the proper selection of K_p and K_i constants a pole zero cancellation can be done resulting in a system whose close loop transfer function is that of a first order system with a simple time constant.

$$Hi_{ol}(s) = \frac{K_{pi}s + K_{ii}}{s} \cdot \frac{1}{Ls + R} \tag{2}$$

B. Outer loops

If the time constant of the inner loop is fast enough it will seem instantaneous to the outer loop control, and the Hi_{cl} can be considered as 1, an example of this simplification can be seen in figure 3 where the v control is presented without the inner control loop. For the power control loop the power is proportional to the current and the voltage which is assumed to be constant as it is set by the grid, see figure 2. For the voltage control loop, the model is slightly more complex as the current flows through a fix load and this sets the voltage, in the dq frame there is an interaction between the currents that cannot be eliminated as it was in the decoupling with the inner loop; therefore, the complementary component of the current act as a perturbation to the system, as observed in figure 3.

$$Hp_{ol}(s) = \frac{K_{pp}s + K_{ip}}{s} \cdot Hi_{cl} \cdot \frac{3}{2}V_d \tag{3}$$

$$Hv_{ol}(s) = \frac{K_{pv}s + K_{iv}}{s} \cdot Hi_{cl} \cdot (L_l s + R_l) \tag{4}$$

After a proper selection of the PI parameters based on the desired response time of the inner and outer loops, and based on the filter characteristics it is observed that the location of the poles for the proposed control loops remains stable in figure 4. The values used for the PI parameters for the simulations are compiled in table II.

VI. Simulations

When the system starts to islanded operation mode the local load is initially powered down. The inverter will start its operation in normal islanded mode and quickly, yet gradually,

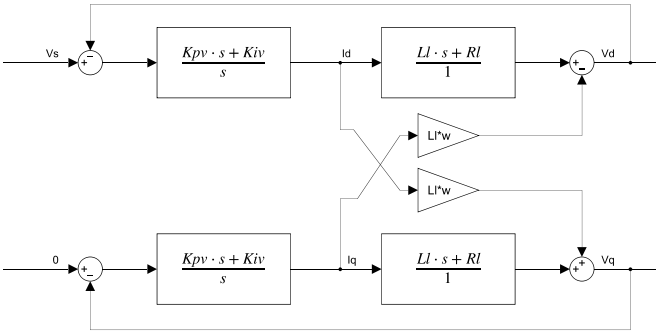

Fig. 3. Model of system and voltage control in the dq frame simplifying the inner current control loop

TABLE II
PI PARAMETERS

Kpi	3	Kii	90
Kpp	$30 \cdot 10^{-6}$	Kip	0.08
Kpv	$60 \cdot 10^{-6}$	Kiv	12

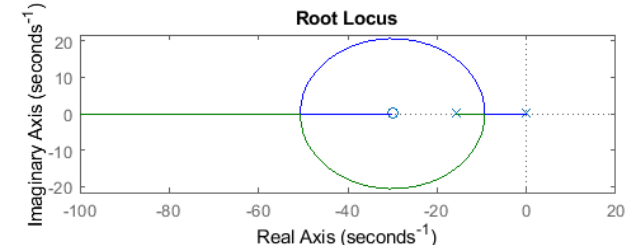

(a) Current control loop

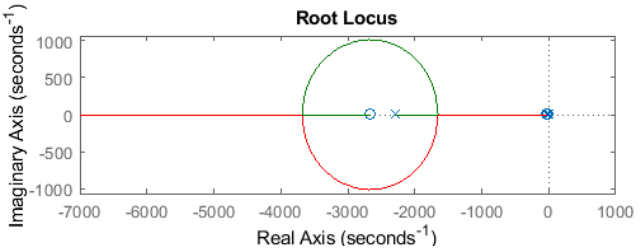

(b) Power control loop

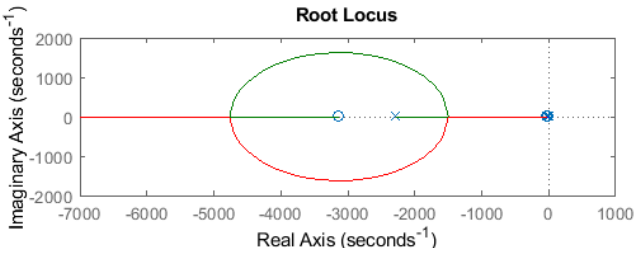

(c) Voltage control loop

Fig. 4. Root Locus of the used control loops

increase the current until the desired voltage is obtained at the output while ensuring its correct alignment with the d

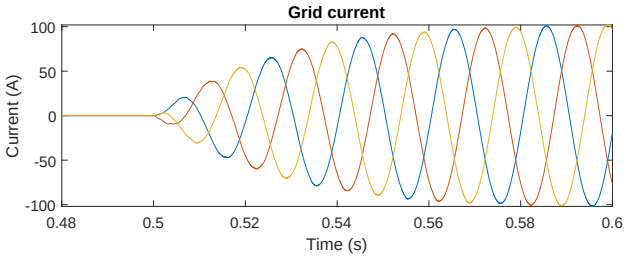

Fig. 5. Current during start to islanded mode

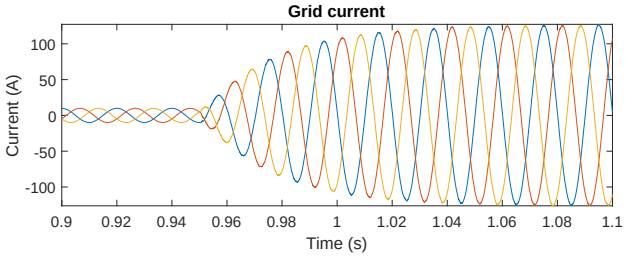

Fig. 6. Current during start to grid-connected mode

axis. The behaviour of the current can be observe in figure 5 where no problems are observed. To start working when the local load is already connected to the grid then the voltage reference given by the controller has to match that of the grid. This is easily achieved activating the RSL and waiting for the synchronization signal, after which the system can be turned on in grid-connected mode. As observed in figure 6, there is an initial current present due to the capacitor from the LCL filter and the current gradually increases to provide the set-point power injection. Again no undesirable behaviours are observed and the start of operations is completely seamless.

If the system is operating in islanded mode and its connection to the grid is desired, then the inverter will begin to quickly synchronize and match voltage, frequency and phase with little to no error. The system can seamlessly reconnect after this process and change its operation mode from islanded to grid-connected. The current smoothly changes to follow the new set-point without any signs that the reconnection ever happened as observed in figure 7c. The frequency of the microgrid varies within the specified limits, in this example between 48 Hz and 52 Hz to achieve the synchronization as observed in figure 7b

If the grid fails during operation the system will be effectively islanded without noticing it. At the moment of the fault the voltage will suddenly rise or drop and the current will rise or drop depending on how the local load compares to the set-points. The overvoltage can be observed in figure 8a. Since the system will be trying to control the power in an islanded system a small misalignment from the voltage will occur which will be reflected in the frequency, by using a small droop during grid-connected mode this error is greatly limited, see figure 8b, and when the grid is recovered at time 2.75 s no overcurrents are observed, see figure 10a. If the islanded condition is sustained, then the AIP [10] detects the fault and disconnects from the grid, going back to a constant frequency

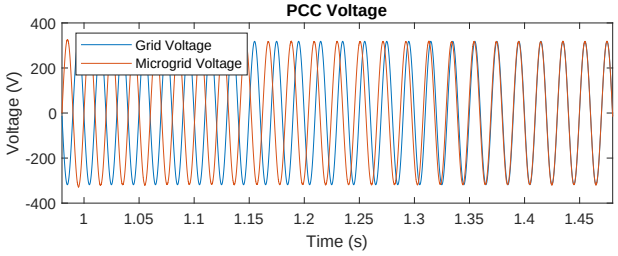

(a) Voltages

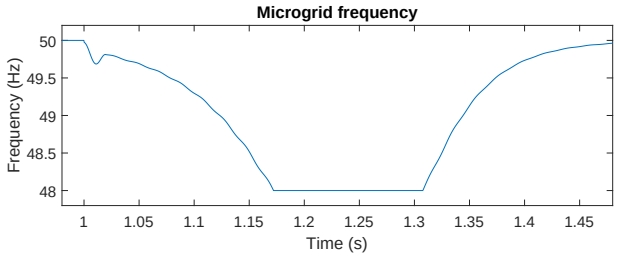

(b) Frequency

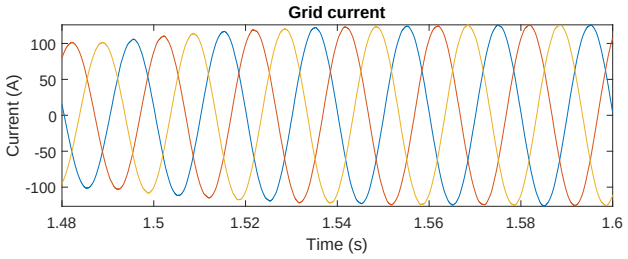

(c) Current during reconnection

Fig. 7. Resynchronization during islanded mode

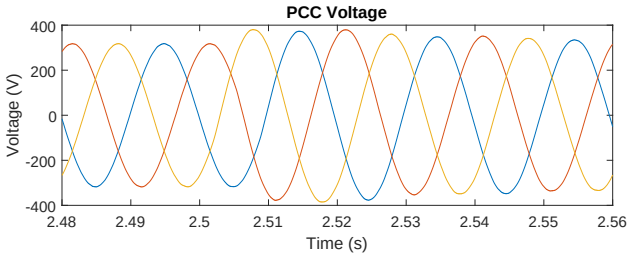

(a) Voltage at fault instant

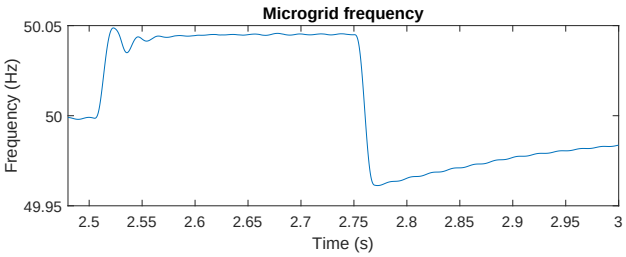

(b) Frequency

Fig. 8. Transient during short grid-loss

reference, see figure 9a.

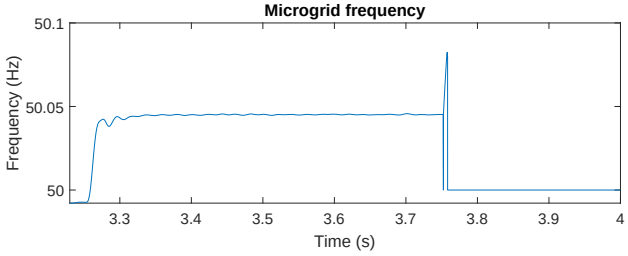

(a) Frequency

Fig. 9. Transient during long grid-loss

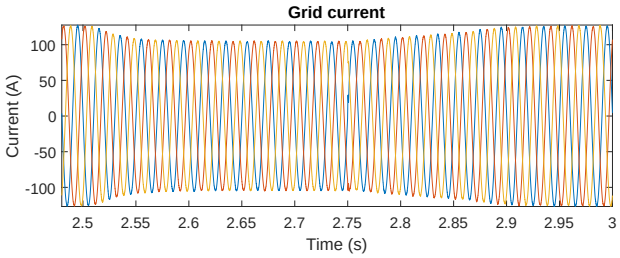

(a) Short grid-loss

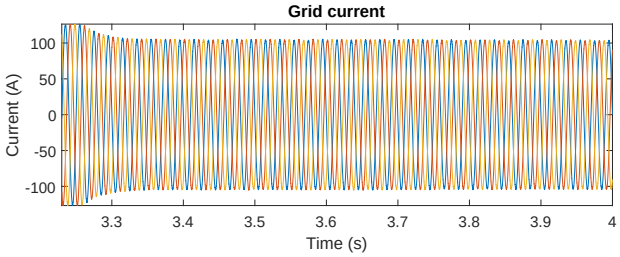

(b) Long grid-loss followed by islanded operation

Fig. 10. Current behaviour during grid-loss

A. *Resynchronization with UDC model*

The UDC resynchronization method proposed in [11] uses a virtual current just like the RSL block used in this paper, so it is a technique with many similarities to the one here presented. A simulink simulation with the UDC was ran to observe its performance during resynchronization. The results from this simulation are as expected similar in both the current and frequency behaviour to the ones obtained with the RSL.

VII. Conclusions

With this implementation of the RSL block in the control of an inverter, a seamless transition was achieved between all operations, this being: start of operations as an island, start of operations in grid connected mode, transition between islanded mode to grid-connected mode and turn off from any operation mode. The transition between grid-connected mode to islanded mode can only be seamless when the local load is known, as the power set-points have to match those of the load to avoid over or under-voltages. Regardless of this, even during faults like the sudden loss of the grid all undesirable behaviours on the current are avoided. The frequency control is robust and works in a stable manner on all operation modes and allows for seamless reconnections in half a second. It was

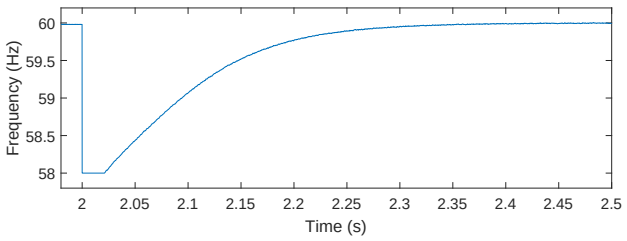

(a) Frequency during synchronization

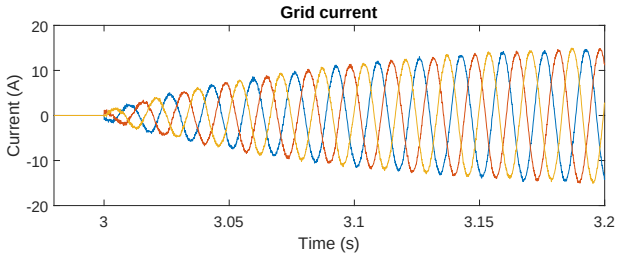

(b) Current during reconnection

Fig. 11. Transient during change from islanded mode to Grid-connected with UDC controller

observed that the results obtained with this control scheme are similar to those of the re-synchronization of UDC [11] with the advantage that by not using a droop control the system works at nominal values while maintaining the robustness and stability provided by not using a conventional PLL block.

REFERENCES

[1] "Microgrid Defined: Three Key Features that Make a Microgrid a Microgrid," Jun. 2020, section: About Microgrids. [Online]. Available: https://microgridknowledge.com/microgrid-defined/

[2] H. Xu, X. Zhang, F. Liu, D. Zhu, R. Shi, H. Ni, and W. Cao, "Synchronization strategy of microgrid from islanded to grid-connected mode seamless transfer," in *2013 IEEE International Conference of IEEE Region 10 (TENCON 2013)*, Oct. 2013, pp. 1–4, iSSN: 2159-3450.

[3] C. Lassetter, E. Cotilla-Sanchez, and J. Kim, "A Learning Scheme for Microgrid Reconnection," *IEEE Transactions on Power Systems*, vol. 33, no. 1, pp. 691–700, Jan. 2018, conference Name: IEEE Transactions on Power Systems.

[4] C. Cho, J. Jeon, J. Kim, S. Kwon, K. Park, and S. Kim, "Active Synchronizing Control of a Microgrid," *IEEE Transactions on Power Electronics*, vol. 26, no. 12, pp. 3707–3719, Dec. 2011, conference Name: IEEE Transactions on Power Electronics.

[5] D. Shi, Y. Luo, and R. K. Sharma, "Active synchronization control for microgrid reconnection after islanding," in *IEEE PES Innovative Smart Grid Technologies, Europe*, Oct. 2014, pp. 1–6, iSSN: 2165-4824.

[6] T. Uten, C. Charoenlarpnopparut, and P. Suksompong, "Synchronization Control for Microgrid Seamless Reconnection," in *2019 14th International Joint Symposium on Artificial Intelligence and Natural Language Processing (iSAI-NLP)*, Oct. 2019, pp. 1–6.

[7] Y. Zhang, R. A. Dougal, and H. Zheng, "Tieline Reconnection of Microgrids Using Controllable Variable Reactors," *IEEE Transactions on Industry Applications*, vol. 50, no. 4, pp. 2798–2806, Jul. 2014, conference Name: IEEE Transactions on Industry Applications.

[8] M. Amin, "A Robust-Synchronization-Loop for Grid-Connected Distributed Generation Converters," in *IECON 2020 The 46th Annual Conference of the IEEE Industrial Electronics Society*, Oct. 2020, pp. 3648–3653, iSSN: 2577-1647.

[9] M. Dursun and M. K. DÖŞOĞLU, "LCL Filter Design for Grid Connected Three-Phase Inverter," in *2018 2nd International Symposium on Multidisciplinary Studies and Innovative Technologies (ISMSIT)*, Oct. 2018, pp. 1–4.

[10] M. Amin, Q.-C. Zhong, and Z. Lyu, "An Anti-Islanding Protection for VSM Inverters in Distributed Generation," *IEEE Open Journal of Power Electronics*, vol. 1, pp. 372–382, 2020, conference Name: IEEE Open Journal of Power Electronics.

[11] M. Amin and Q.-C. Zhong, "Re-synchronization of Universal Droop Control Distributed Generation Inverter to the Grid," in *2019 IEEE Energy Conversion Congress and Exposition (ECCE)*, Sep. 2019, pp. 4435–4440, iSSN: 2329-3748.